Since January 2020 Elsevier has created a COVID-19 resource centre with free information in English and Mandarin on the novel coronavirus COVID-19. The COVID-19 resource centre is hosted on Elsevier Connect, the company's public news and information website.

Materials Science & Engineering R 143 (2021) 100594

Contents lists available at ScienceDirect

Materials Science & Engineering R

journal homepage: www.elsevier.com/locate/mser

Electrospun ultrafine fibers for advanced face masks

Zhenfang Zhang [a], Dongxiao Ji [a,*], Haijun He [b], Seeram Ramakrishna [a]

[a] Faculty of Mechanical Engineering, National University of Singapore, 117574, Singapore
[b] Department of Polymer Engineering, Faculty of Mechanical Engineering, Budapest University of Technology and Economics, Műegyetem rkp. 3-9, H-1111, Budapest, Hungary

ARTICLE INFO

Keywords:
Virus
Mask
Respirator
Filtering mechanism
Nanofibers
Reusable mask
COVID-19
SARS-CoV-2

ABSTRACT

The outbreak of Coronavirus Disease 2019 (COVID-19), which is caused by severe acute respiratory syndrome coronavirus 2 (SARS-CoV-2), has triggered great global public health concern. Face masks are essential tools to reduce the spread of SARS-CoV-2 from human to human. However, there are still challenges to prolong the serving life and maintain the filtering performance of the current commercial mask. Filters composed of ultrafine fibers with diameter down to tens of nanometers have the potential to physically block viruses. With adjustable composition and nanostructures, the electrospun ultrafine fiber filter is possible to achieve other necessary functions beyond virus blocking, such as antiviral, transparent, and degradable, making it an important part of fighting the epidemic. In this review, beginning with the basic information of the viruses, we summarize the knowledge of masks and respirators, including the filtering mechanism, structure, classification, and standards. We further present the fabrication method, filtering performance, and reusable potential of electrospun ultrafine fiber-based masks. In the end, we discuss the development directions of ultrafine fibers in protective devices, especially their new functional applications and possible contributions in the prevention and control of the epidemic.

1. Introduction

The unprecedented swift spread of the coronavirus disease 2019 (COVID-19), caused by severe acute respiratory syndrome coronavirus 2 (SARS-CoV-2) [1], has become a great global public health concern in 2020 [2,3]. The SARS-CoV-2 may result in severe pneumonia, acute myocardial injury, and chronic damage to the cardiovascular system [4] with a mortality rate ranging from 3 to 5% [5]. As of 24 September 2020, the pandemic has caused more than 31,872,860 confirmed cases carrying more than 974,023 reported deaths in 215 countries and territories worldwide. It has a strong human-to-human transmission ability [6] mainly by inhalation or contact with infected droplets [7]. Before an effective vaccine is developed and can be widely accessed, wearing a mask in the community is one of the most effective measures to decrease the spread of viruses [8]. This situation makes the mask a national essential. However, the currently commercial masks, using melt-blown polypropylene (PP) non-woven fabric as a filter layer, are designed to be used for a few hours and dispose of responsibly. As masks protect people from the viral infection, there is a worldwide surge in the use of billions of face masks every day. This accentuated the worldwide shortages of masks [9]. Although homemade masks or disinfecting masks may ease the shortage situation, there are no scientific evidences to confirm their effectiveness. In the long term, functional masks, such as reusable masks or anti-virus masks, will hopefully solve the dilemma of mask shortages. Reusable masks will extend the life of the mask while maintaining the filtration efficiency, and anti-virus masks will kill the virus on the mask in time to prevent secondary infection caused by virus retention [10]. The development of novel masks will help us cope with the epidemic situation similar to COVID-19.

Ultrafine fibers [11], whose width is measured in nanometers, are highly regarded in air filtration applications because of their high surface area and small inter-fiber pore sizes [12]. The ultrafine fibers are a natural fit for masks and protective textiles, as high air permeability is desired to improve user comfort [13]. Melt-blown Polypropylene(PP) non-woven fabrics with a fiber diameter of 0.5–10 um are wildly used in current masks [14]. Their relatively large diameter is insufficient to efficiently filter 0.3 um particles or aerosols [15]. In this regard, electrostatic treatment is needed to improve filtration efficiency. However, during wearing or cleaning, static electricity is easily lost. Thus these masks are disposable. This not only caused a waste of resources but also

* Corresponding author.
E-mail address: mpejid@nus.edu.sg (D. Ji).

https://doi.org/10.1016/j.mser.2020.100594
Received 29 July 2020; Received in revised form 30 September 2020; Accepted 14 October 2020
Available online 20 November 2020

exacerbated the shortage of masks during the epidemic. Electrospun nanofiber membranes with fiber diameter below 0.3 um are promising alternative candidates for serving as reusable filters. They achieve physical barriers to particles and viruses through smaller fiber diameters and pore diameters, getting rid of the limitation of static electricity. When using appropriate disinfection methods without destroying their physical structure, the nanofiber membranes are able to be reused. Furthermore, the functionalization of fiber filter materials can be achieved by rationally designing the composition and structure of ultrafine fibers, helping us to better respond to the spread of the virus.

This review will firstly introduce the information of the virus with a special focus on SARS-CoV-2. We then summarized the filtering mechanism, structure, classification, and standards for masks and respirators. Additional parts highlight the fabrication method, filtering performance, and reusable potential of electrospun nanofiber-based masks. In the end, we discuss the development directions of ultrafine fibers in protective devices, especially their new functional applications and possible contributions in the epidemic like COVID-19.

2. Viruses and their transmission

The virus is an original biological entity that has a single type of nucleic acid (DNA or RNA) [16]. This specific structure opposes the virus to living organisms with a cellular structure (prokaryotes and eukaryotes) [17]. The nucleic acid, which may be single-stranded or double-stranded [18], is packaged in a capsid composed of either protein or a lipid membrane and protein [19]. The size of the virus varies from 20−300 nm [20]. Generally, the virus reproduces from its genetic material by replication within the host cell during attachment, entry, translation, transcription/replication, assembly, and release successively [21]. These processes will cause a strong immune response in the host, leading to absolute intracellular parasitism.

The human body is a diverse ecosystem that contains hundreds of trillions of microbes (bacteria, fungi and viruses) [22] which might be or become pathogenic under certain circumstances. Transmission happens when the virus interacts with the human body through the surface of a material [23]. The transmission of the virus from human-to-human can be classified into horizontal transmission and vertical transmission [24]. The horizontal transmission mainly includes respiratory (mainly droplets or airborne), alimentary tract (food and water), wound skin (insect bite), sexual and blood (transfusion, injection, and organ transplantation) transmission [25]. The vertical transmission mainly through the pregnant way that the virus is transmitted to the infant [26].

Ever since the Tobacco Mosaic Virus(TMV) was first discovered by Dmitri Ivanovsky in 1886 [27], more than 5000 types of viruses have been recognized [28]. Among them, viruses with human-to-human transmission properties usually pose a huge impact on human civilization. Some representative human-to-human transmission virus were listed in Table 1.

Phylogenetic analyses of the coronavirus genomes have revealed that SARS-CoV-2 is a member of the *Betacoronavirus* genus [29]. The SARS-CoV-2 is a novel enveloped beta-coronavirus with a single-stranded positive-sense RNA genome [30]. It mainly contains spike glycoprotein (S), RNA, envelope, and hemagglutinin-esterasedimer (HE) (Fig. 1). SARS-CoV-2 entry into host cells through the mediating of transmembrane spike (S) glycoprotein that forms homotrimers protruding from the viral surface [31]. A Recent study indicated that SARS-CoV-2 S uses angiotensin-converting enzyme 2(ACE2) to enter human cells, correlating with the efficient spread of SARS-CoV-2 among humans [29]. The clinical manifested that most cases infected by SARS-CoV-2 were mild cases (81%), whose symptoms were usually self-limiting and recovery in two weeks [32]. While severe patients progressed rapidly with acute respiratory distress syndrome (ARDS) and septic shock, eventually ended in multiple organ failure, which usually occurred for the elderly and those with comorbidities [33]. Furthermore, the SARS-CoV-2 has a strong ability of rapid development and human-to-human transmission which mainly through respiratory (inhalation) [2]. The virus is released into the air in the form of droplets (diameter $>$ 5 um) or aerogel (diameter $<$ 5 um) when the infected people breathes, coughs, or even sneezes. The virus can spread in 3–6 feet from an infected person with the form of droplets [34]. While for airborne transmission, which is a significant route of infection in indoor environments [35], the virus can travel as far as 30 feet or more [36]. Moreover, SARS-CoV-2 is infectious within 30 min [36] to 16 h

Table 1
Representative human-to-human transmission viruses in recent years.

Virus name	Origin	Characteristics	Case-fatality rate/Harm	Prophylaxis or vaccine	Human-to-human transmission	Transmission method	First breakout	Epidemic areas
Ebola virus	Unknown	RNA virus, 80 nm in diameter, length up to 14,000 nm	50%-90%	No	Yes	Direct contact blood, fluid of the patient	Africa in 1976	Africa
A(H1N1) virus	Pig	RNA virus, 120 nm in diameter	6.77%	No	Yes	Droplet and contact transmission	Mexico or USA in 2009	Worldwide
SARS-CoV-1	Chrysanthemum bat	RNA virus, 60−220 nm in diameter	14%	No	Yes	Droplet and contact transmission	China in 2003	Worldwide
HIV	Gorilla and chimpanzee	RNA virus, 120 nm in diameter	Almost 100%	No	Yes	Sexual contact across mucosal surfaces, maternal-infant exposure, percutaneous inoculation	USA in 1981	Worldwide
SARS-CoV-2	Unknown	RNA virus, 60−140 nm in diameter	3%−5%	No	Yes	Droplet and contact transmission	China in 2019	Worldwide
Zika virus	Unknown	RNA virus, 20 nm in diameter	Infants with microcephaly	No	No	Aedine mosquitoes	Africa in 1947	Worldwide (Mainly in Brazil)
Marburg virus	Unknown	RNA virus, 800−14000 nm in length	25%~100%	No	Yes	Contact transmission	Africa in 1967	Worldwide
MERS-CoV	Unknown	RNA virus, 120−160 nm in diameter	35%	No	Yes (difficult)	Contact transmission	Saudi Arabia in 2012	Mainly in Saudi Arabia, Arab emirates, Korea

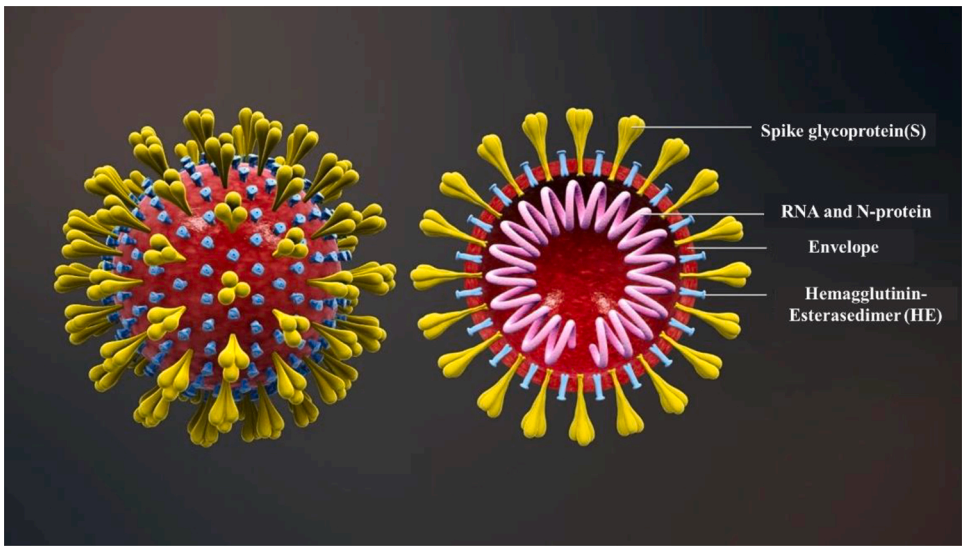

Fig. 1. The structure of SARS-CoV-2. Reproduced with permission from [44]. Copyright 2020, http://www.seebio.cn/Article/1_1.html.

[37] after being released into the air.

The high infectivity of SARS-CoV-2 is also related to its strong survivability on inanimate surfaces [40]. The stability of virus-containing aerosols on common inanimate surfaces may be flexible considering the materials landed, environmental temperature and humidity, etc. The aerosol containing SARS-CoV-2 has significantly longer stability on a smooth surface than a coarse surface [37]. Holbrook et al. investigated the surface stability of SARS-CoV-2 in five environmental conditions, including plastic, stainless steel, copper, and cardboard, using a Bayesian regression model [38]. It was concluded that the SARS-CoV-2 is remarkably stable on plastic and stainless steel, viable up to 72 h as compared to copper (up to 4 h) and cardboard (up to 24 h). Chin et al. measured the stability of SARS-CoV-2 on different surfaces at room temperature (22 °C) with a relative humidity of 65% [39]. The experiment indicated that the virus is still infectious within 3 h after it is implanted on printing paper and toilet paper, and this infectiousness can remain on wood and clothing for at least two days. It worth noting that the virus can still be detected on the outer layer of a surgical mask after 7 days.

Additionally, SARS-CoV-2 can survive longer in the environment of lower temperatures and lower relative humidity [37]. Chan et al. found that dried SARS-CoV-2 virus can retain viability for over 3–4 days on glass at room temperature and 14 days at low temperature (4 °C), whereas it will lose viability rapidly within one day at the relatively higher temperature (37 °C) [40]. Kratzel et al. further demonstrated that SARS-CoV-2 infectivity had a sharp reduction during the drying process. However, it will remain infectious for several days in a dried condition regardless of the temperature [41]. Moreover, SARS-CoV-2 also show high stability in a wide range of pH values (pH 3–7) at room temperature [39]. These results highlight SARS-CoV-2's high survivability and the difficulty of prevention and control.

In this regard, it is essential to use appropriate personal protective equipment (PPE), including face masks and respirators, to prevent exposure and potential infection. The case-control study in 2003 SARS-CoV-1 indicated that masking was a continuous form of protection to stop the spreading of saliva and respiratory droplets, with a 70% risk reduction compared to those not wearing a face mask [42]. Therefore, the use of a face mask may serve as source control by preventing dispersal of droplets during talking, sneezing, and coughing [43], as well as reduce the risk of environmental contamination by SARS-CoV-2.

3. Face masks

3.1. Classification and standards of face mask

The loose-fitting face masks can be classified into isolation, procedure, laser, dental, medical, and surgical masks [45]. These are generally expected to prevent the exposure of nose and mouth in fluids or large droplets which may exist in the environment, as well as to contain respiratory secretions of the wearer. The surgical masks are cleared for use as medical devices by the USA Food and Drug Admission (FDA), or equivalent agencies outside the USA. Distinct from the face masks, the respirators in our context protect wearers from certain levels of contaminants in the air in the form of half-face or full-face masks [45]. The respirators are always tight-fitting due to the filtering performance strongly depending on the fitting. Respirators' performance characteristics are tested at national regulatory standard conditions [46]. The requirement for N95 (United States), KN95 (China), P2 (Australia/New Zealand), DS (Japan), Korea 1st class (Korea) and FFP2 (EU) are similar in filtration efficiency. The N95 mask is one of nine anti-particulate masks certified by National Institute of Occupational Safety and Health (NIOSH) [47]. "N" means unsuitable for oily particles (the soot produced by cooking is oily particles, and the droplets produced by people speaking or coughing are not oily); "95" means the filtering efficiency under the designated testing conditions can reach 95%. N95 is not a specific product name. As long as the product meets the N95 standard and passes the NIOSH review, it can be called a certified ``N95 mask''. The major international masks and respirator's standards are listed in Table 2. The appropriate use of face masks or respirators is able to protect an individual from exposure and potential infection of respiratory transmission and body fluids [45,48].

With the increase of BFE, PFE, Delta P (delta differential pressure breathability) and FRP (fluid resistance pressure) of face masks and respirators, the comprehensive protective performance will be higher. Masks should be fluid resistant when used for medical purposes [49]. The healthcare workers must wear medical-grade masks and respirators to prevent the exposure toward a high-concentration virus environment. For the public, the WHO has recently issued a recommendation for the widespread use of face masks as an essential strategy to protect against COVID-19 [50]. In case of the shortage of filtering face-piece respirators, the surgical mask is recommended to protect individuals in public while maintaining comfort to reduce the spread of respiratory infections caused by virus like SARS-CoV-2 [51]. Once the masks/respirators are to be used after made, they must be tested to ensure their safety in various

Table 2
The major international mask and respirator standards.

Device name	Splash resistance	Type of protection	Filter performance	Equivalent classes	Fit-test	Standards
Medical face mask	NO YES	Droplets	Variable	Level 1/Type I/ Type II Level 2/ Level 3/ /Type IIR	Not needed	YY/T0969−2013(China) YY0469−2011(China) Class 1/ Class 2/Class 3
Respirator	YES	Droplets and airborne particles	≥80%	FFP1	Needed	GB 19083−2010 (China)/ Level 1/Level 2/Level 3/N95/N99/N100/P96/P99/P100/R95/R99/R100: ASTMF2100−2019(US) Type I/ Type II/ Type IIR/FFP1/FFP2/FFP3: EN14683−2019(UN) KN90/KN95/KN100 KP90/KP96/KP100: GB 2626−2006(China)
			≥94%	Class1/FFP2/N95/P95/R95		
			≥99%	Class2/Class3/FFP3/N99/N100/P99/P100/R99/R100		
	NO	Droplets and airborne particles	≥80%	FFP1/DL1/ DS1/KF80		FFP1/ FFP2/ FFP3: EN 149−2001(UN)
			≥90%	KN90/ KP90		
			≥94%	KN95 /N95/FFP2 / DL2/ DS2/ P2/ R95/ KP95/P95		N95/N99/N100 /R95/R99/R100/P95/P99/P100: CFR 42−84-1995(US) DS1/DS2/DS3/DL1/DL2/DL3: JIS T 8151−2018 (Japan) KF80: KS M 6673−2008(Korea) AS/NZS 1716−2012 (Australia/New Zealand)
			≥99%	N99/FFP3/KF99/ R99/ KF99/ P99		
			≥99.97%	KN100/N100/ R100/ KP100/ P100/ DL3/ DS3/P3		

situations. Concerning the epidemic COVID-19, we also shed light on the test method of antiviral activity. They are listed in the Table 3.

An organization that wants to market masks or respirators need to get the clearance or approval from relevant government departments, such as 510(k) clearance [52] for surgical masks, NIOSH approval for respirators in the United States and European Conformity (CE) [53]. Taking the United States as an example, a manufacturer marketing a surgical mask imported from outside the United States should conform to the general controls of the FDA and Cosmetic Act (the Act), including the premarket notification requirements described in 21 CFR 807 Subpart E [54], and obtain a substantial equivalence determination from FDA prior to marketing the device [55], which states that the surgical mask can be marketed in the U.S. Generally, 510(K) clearance, a premarket submission made to FDA to demonstrate that the device to be marketed is as safe and effective [56], is needed while a Premarket Approval application (PMA) is not required [52].

Currently, the FDA's Enforcement Policy and relevant Emergency Use Authorizations (EUAs) for face masks are established to increase the supply of face masks and similar devices during the epidemic [57]. If a face mask meets the appropriate requirements and recommendations, it is up to the manufacturer whether wish to market the device under the enforcement policy or under the EUA. Surgical masks should meet fluid-resistance testing consistent with the ASTM Standard F1862 and address flammability, either through testing or labeling [58]. If surgical masks including the liquid barrier testing and labeling recommendations meet the requirements in the Enforcement Policy, the 510(K) submission and other requirements may not need during the public health emergency [59]. Moreover, an N95 filtering facepiece respirators (FFRs) need to be approved as N95 respirators by NIOSH first and then cleared by the FDA for fluid resistance and flammability properties [60]. Meanwhile, a EUA is not needed for surgical masks to market as long as the recommendations in the Enforcement Policy Guidance Document are followed [61].

3.2. Structure of commonly used surgical mask

A typical surgical mask is composed of at least three layers of nonwovens made by PP fibers: the cover layer, filter layer and shell layer (Fig. 2a). The cover layer is usually hydrophobic, and the shell layer supports the filter layer and makes people feel comfortable. These two layers are spun-bond nonwovens or hot-air nonwovens with a fiber diameter of 15−40 μm. They have small contributions to the overall filtration efficiency [62], but they show high strength and good air permeability. The filter layer consists of melt-blown non-woven fabric with a diameter of 0.5–10 microns (Fig. 2b, c), which plays a major role in filtering. Their relatively large diameter is insufficient to efficiently filter 0.3 um particles or aerosols [63]. In this regard, electrostatic treatment is needed to improve filtration efficiency (Fig. 2d). However, during wearing or cleaning, static electricity is easily lost. Generally, the filtration efficiency of this kind of filter will greatly reduce after long-time wear or undergo other post-treatment. The filtration efficiency will improve with the increase of thickness of the filter layer, normally at the cost of air resistance. To meet the ideal performance of a face mask, the characteristics of the mask should balance high filtration, adequate breathability and fluid penetration resistance [50]. The filter layer keeps great protection against floating particles and the cover layer has significant resistance to fluid. In the meanwhile, the mask across all the layers must ensure unhindered breathing during inhalation and exhalation (Fig. 2e).

3.3. Filtration mechanism of fiber filter

The air filtration mechanism of fiber filter is mainly based on physical filtration mechanism (PFM), including interception, inertial impact, diffusion, gravitation, and electrostatic attraction (Fig. 3) [65]. During a particle filtration process, an interception occurs when the particle radius is equal to or larger than the fiber-particle distance (within the particle size range of 0.1−1 μm) [66]. The particles are immediately blocked outside the masks once they come in contact with and stick to the fiber following the air streamline around the fiber. Inertial impact happens when a particle is bigger than 1 μm with a large mass, which is unable to follow the curve paths of the air streamline colliding into the fiber. Especially for the particles in high velocity, it is more difficult to pass through the mat pores of the mask sieve and to reach the wearer. The diffusion mechanism [67] causes aerosol particles to deviate from their original flow lines randomly when they are near the fibers, particularly for small particles with sizes below 0.1 μm. The electrostatic attraction happens in the filters which are made up of electrostatically charged mats [68]. The oppositely charged particles are attracted via electrostatic driven adsorption. The electrostatic attraction is quite effective for capturing sub-micron particles without the increase of pressure drop because the web structure won't be altered [69]. However, the filtration conditions will change when the fibers of the filter are within nanoscale. The aerodynamic behavior of airflow around the

Table 3
The testing methods of surgical mask and respirator.

Test index	Definition	Test methods
Bacterial Filtration Efficiency (BFE) (BS EN 14683−2019/ ASTM 2101)	The effectiveness in preventing the passage of aerosolized bacteria, expressed in the percentage of a known quantity that does not pass the medical face mask material at a given aerosol flow rate.	The test works by shooting an aerosol with a liquid suspension of Staphylococcus aureus bacterial at the mask at 28.3 L per minute. Challenge controls are maintained at 1700−2700 colony forming units (CFU) with a mean particle size of 3 ± 0.3 μm.
Differential Pressure (Breathability) (BS EN 14683−2019/ GB 19083−2010)	Air permeability of the mask, measured by determining the difference of pressure across the under specific conditions of air flow, temperature and humidity.	To ensure the mask will hold its shape and have proper ventilation while the wearer breathes, breathing resistance is tested by shooting a flow of air at it, then measuring the difference in air pressure on both sides of the mask by a water-filled differential manometer.
Splash Resistance (ISO 22609−2004/ ASTM F1862)	Ability of a medical face mask to withstand penetration of synthetic blood projected at a given pressure.	A volume of synthetic blood is sprayed horizontally at the specimen to simulate the scenario of a mask being splashed by a punctured blood vessel to ensure the liquid cannot penetrate and contaminate the wearer.
Particulate Filtration Efficiency (PFE) (ASTM F 2299/ EN 149−2001)	The efficiency of the filter material in capturing aerosolized particles smaller than one micron, expressed as the percentage of a known number of particles that does not pass the medical face mask material at a given flow rate.	Also known as the latex particle challenge, this test involves spraying an aerosol of polystyrene microspheres at 28.3 L per minute to ensure the mask can filter the size of the particle it's supposed to.
Flammability (16 CFR Part 1610)	The characteristics of a material that pertain to its relative ease of ignition and relative ability to sustain combustion.	Since several elements of an operating room can easily cause fire, the surgical masks are tested for flammability by being set on fire to measure how slowly it catches and how long the material takes to burn.
Antiviral Activity (BS ISO 18184−2019)	Property of any substance (chemical or otherwise) producing a modification of one of the elements of the virion structure which induces the latter's inability to replicate.	The test is conducted by comparing the reduction rate of virus between specimen and remaining infectious virus. Plaque assay and TCD50 methods are available to quantify the infectious virus tire.

periphery of ultrafine fibers would change dramatically [65]. Besides, the strong Van der Waals forces which are capable of adsorbing submicron-sized particles will generate [12]. The diffusion, inertial impact, and interception will also be enhanced due to the good interconnectivity of the pores.

3.4. Weaknesses of the commonly used mask

The PP filter plays a key role in the filtration performance of the common mask. The charge retention capacity and stability of the filter is critical as the filtration efficiency is influenced greatly by the strength of the electric field generated within the fibrous filter [70]. The electret filter can be fabricated via charging techniques such as corona charging, tribocharging, and electrospinning [71]. However, the charges will decay gradually during long-term storage or use. This is referred to as dipole charges and inevitable charge dissipation [72]. Accordingly, the commonly used mask is disposable. Recyclability of the discarded mask is also becoming a big challenge for the environment. Regarding these significant problems, it is urgent to develop advanced face masks, such as reusable, antivirus, and degradable masks.

4. Electrospun ultrafine fibers for reusable face masks

4.1. Advantages of ultrafine fibers

Ultrafine fiber provides a connection between the nanoscale world and the macroscale world; the diameter is in the nanometer range while the length is a few hundred microns [73]. They have unique properties such as extremely high surface-to-volume ratio [74], diverse surface chemistry [75] and the ability to form high and interconnected porosity [76]. Compared with conventional micro-fibrous filters (Fig. 4a, b) [77], the filters containing ultrafine fibers significantly increase the possibilities of particulate matter deposition. These advantages could avoid the secondary pollution caused by the particle shedding/leaking. Therefore, the ultrathin fibrous filters are capable of physically blocking ultra-small particles and viruses without the limitation of losing static electricity.

4.2. Fabrication of ultrafine fibrous filter

Electrospinning is a versatile and viable technique for generating ultrafine fibers from polymer solutions or melts [79]. The diameters of electrospun fibers ranging from several micrometers down to a few nanometers, and mostly in hundreds of nanometers have been reported [80]. Typically, the major components of the electrospinning setup include a high-voltage power supply ranging 5−30 kV, a syringe pump, a spinneret, and a conductive collector (Fig. 5a) [81]. During the electrospinning process, the liquid is firstly extruded from the spinneret to form a pendant droplet [79]. Then the charged droplet is deformed into Taylor cone [82]. The jet will form when the voltage exceeds a critical value [83]. In the next, the jet is stretched and accelerated in a straight line and undergoes a whipping instability to split into ultrafine fluids. Ultrafine fibers generate on stationary or revolving grounded metallic targets as the solvent evaporates and the fluids solidify [84]. The diameters of ultrafine fibers can be controlled by adjusting the spinning nozzles, polymer solutions, the fiber collection time, the electric field, etc. For example, Shin et al. fabricated ultrafine fiber whose diameter was thinner than the initial jet of 1300 times due to adjusting stretching and solvent evaporation [85]. The ultrafine fibers can be collected into random nonwoven mats and aligned or meshed structures (Fig. 5b) [81]. Recently, electrospinning has been considered as viable in the encapsulation of bioactive agents to improve their biocompatibility and bioaccessibility, including hydrophobic small substances, hydrophilic small substances and macromolecular active substances (e.g., enzymes, active proteins, probiotics) [86]. This technology has wide applications in filtration, wound dressing [87], drug delivery [88], tissue engineering [89], protective clothing, etc. However, there are manufacturing difficulties associated with the bioactive electrospun nanofibers. For example, the ability of electrospinning of pure proteins is limited due to the complex secondary and tertiary configurations, although proteins have been promising biopolymers for electrospun fiber generation [90]. The manufacturability of bioactive electrospun nanofibers is listed in Table 4.

We propose one possible method to make such an electrospun ultrafine fibrous mask. It is directly coating functional ultrafine fibers on the cover layer of the mask (Fig. 5c, d). To be specific, a soft fiber/ultrafine fiber hybrid filter can be fabricated by coating electrospun ultrafine fibers on the soft fiber layer to replace the filter layer and cover layer in the conventional PP filter mask. In the proposed structure, the

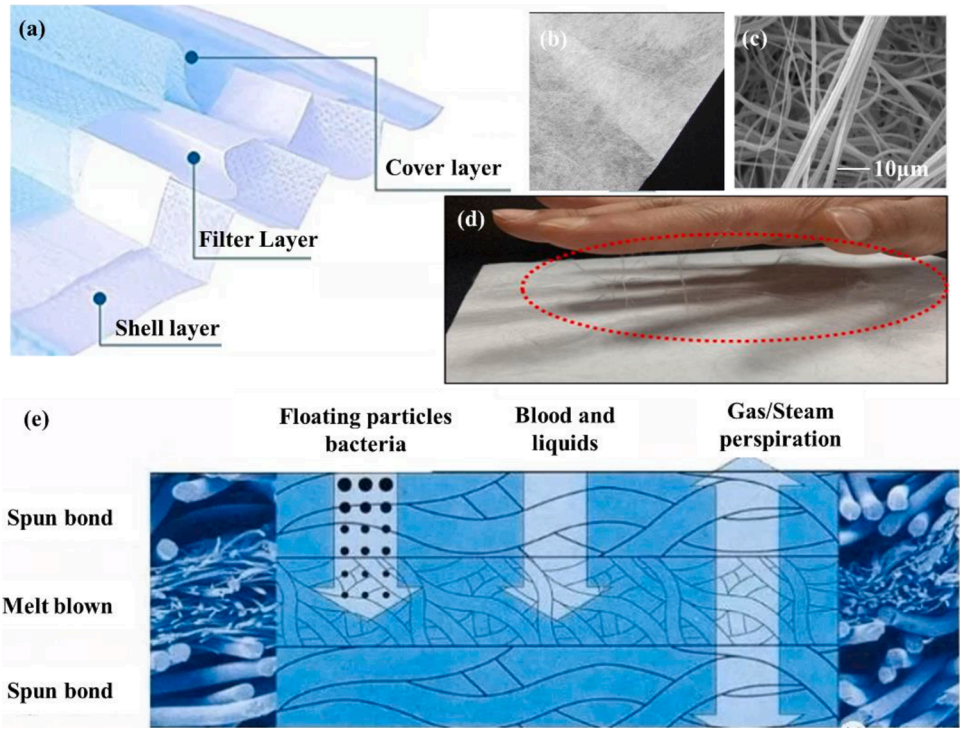

Fig. 2. (a) Diagram of the structure of a surgical mask. (b) Digital photo of the PP melt-blown cloth. (c) SEM image of melt-blown PP fibers. (d) Observation of static charge on the surfaces of melt-blown PP filters. Reproduce with permission from [64]. Copyright 2020, ACS Applied Nano Materials. (e) Schematic diagram of the filtering functions of the three layer.

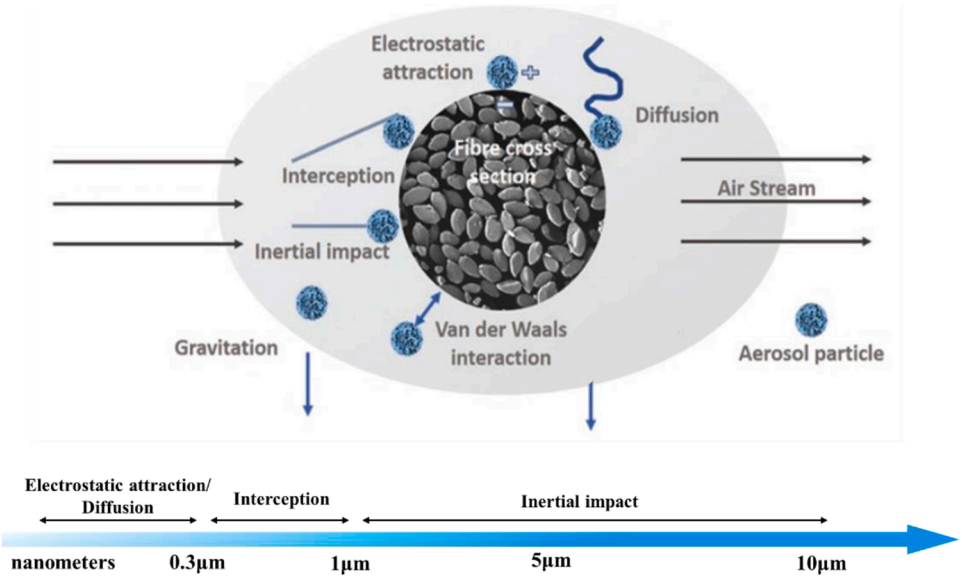

Fig. 3. Filtration mechanism of fiber filter based on the particle size. Reproduced with permission from [65]. Copyright 2019, ACS Applied Nano Materials.

hybrid filter will act as both a filter and a hydrophobic layer. It will show higher filtration efficiency while reducing weight. Additionally, because ultrafine fiber uses a physical barrier method for filtering, this mask has the potential to be reused after disinfection.

4.3. Filtering performance

The ultrafine fibers have demonstrated prospects in creating high-performance filters. Many kinds of ultrafine fibrous filters have been developed with the capabilities to achieve high-efficiency filtration of particles bigger than 10 nm. Omori et al. fabricated high-performance air filters composed of a hybrid structure of nanofiber/microfiber using wet paper processing [107]. The hybrid filters respectively exhibited high performance with quality factor Q_f (Q_f is a widely used index that indicates the filtration performance due to pressure drop) values of 0.043 for nanofiber with average diameters of 180 nm can be achieved for filtering 100 nm particles. Recently, Liu et al. developed self-polarized polyvinylidene fluoride(PVDF) nanofiber/net filters with 2D networks and superior surface adhesion via an innovative in situ electrets electrospinning/netting technique [108]. In this work, the synergistic effect of sieving and adhesion for $PM_{0.3}$ (particle size below 0.3 μm) was enhanced by introducing true nanoscale diameter

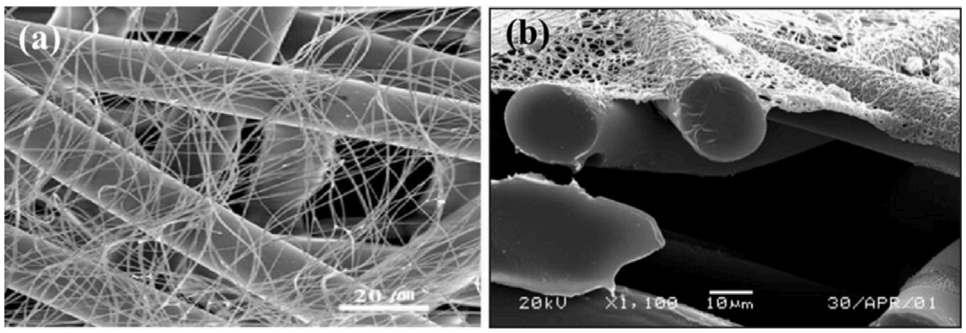

Fig. 4. (a) Comparison of electrospun fiber and PP fiber. (b) SEM image of cross-section of nanofibers on a polyester spun-bond substrate. Reproduced with permission from [78]. Copyright 2003, International Nonwovens Journal.

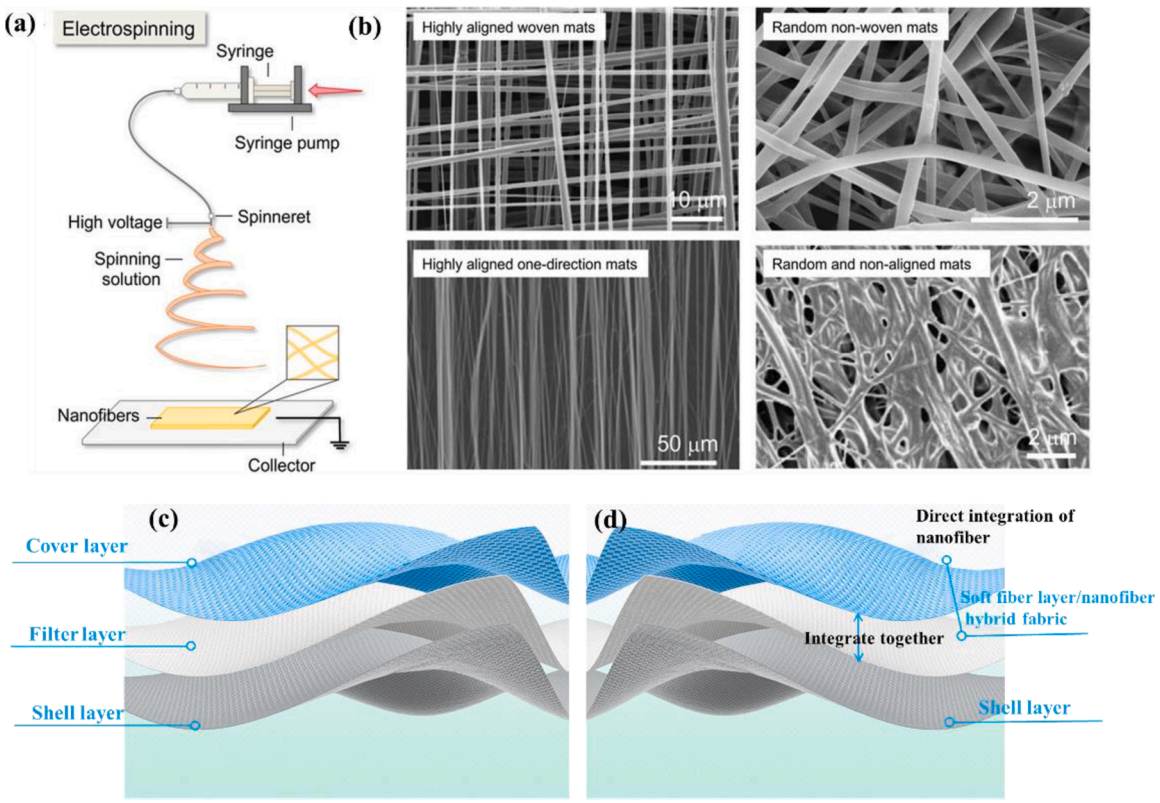

Fig. 5. (a) Schematic diagram of electrospinning technology. (b) SEM images of electrospun nanofibers with different geometries and styles. Reproduced with permission from [81]. Copyright 2020, Advanced Fiber Materials. (c) Structure of commonly used masks. (d) The proposed structure of electrospun ultrafine fibrous masks.

(≈21 nm), small pore size (≈0.26 μm), and highly electret surface (6.8 kV potential) into the 2D nano-nets. The filters enabled the high-efficiency (≈99.998%) capture of $PM_{0.3}$ with super lightweight while maintaining low air resistance (≈0.1% atmosphere pressure), and showed integrated properties of superhydrophobicity and desirable transparency (91%). Similarly, Zhang et al. created spider-web-inspired $PM_{0.3}$ filters based on self-sustained electrostatic nanostructured networks using a unique electrospraying-netting technique [109]. The spider-web-inspired network generator (SWING) filters showed the exceptional long-range electrostatic property and exhibited high efficiency (>99.995% $PM_{0.3}$ removal), low air resistance (<0.09% atmosphere pressure) and high transparency (>82%) in combination with their steiner-tree-structured pores (size 200−300 nm) consisting of nanowires (diameter 12 nm). Moreover, the ultrafine fibrous filters are highly effective in blocking viruses [110], including human influenza H1N1, avian influenza H5N1, SARS-Cov-1, etc. This may be equally valid for SARS-CoV-2. The protective scopes diagram to compare the filtering capabilities of ultrafine fibrous filters, N95 respirators and commonly used surgical facemasks is shown in Fig. 6.

4.4. *Reusable potential of ultrafine fibrous filters*

A reusable mask is expected to maintain effectively after long-time use in a high-moisture environment or after disinfection. Most nanofiber filters, such as polyacrylonitrile(PAN) [111], poly (ε-caprolactone) (PCL) [112] and poly (vinylidene fluoride)(PVDF) [113,114], can withstand water washing and alcohol sterilization. Recently, Ullah et al. compared the melt-blown filter with nanofiber filter through cleaning them with 75% ethanol to evaluate their reusability [64]. According to the comparative evaluations, the nano-filters can be reused multiple times with robust filtration efficiency. Furthermore, Liang et al. prepared a nanofiber-based air filter with thermoplastic polyurethane

Table 4
The manufacturability of bioactive electrospun nanofibers.

Polymer type	Polymer features	Applications	Bioactivity of electrospun nanofibers	Manufacturability
Synthetic polymers				
Poly(vinyl alcohol) (PVA)	Nontoxic, biodegradable, water-soluble and biocompatible.	Immobilization of α-amylase in ultra-fine (PVA) fibers [91];	Immobilized enzyme in PVA fibers showed greater enzymatic activity than the free form and Larger stability at extreme temperature/ PH.	√Blend electrospinning; √Good production capacity; √Morphological fiber change: flatter and thicker; √No bead.
		Encapsulation of gallic acid into PVA fibers. [92]	High antioxidant activity and great thermal resistance > 200 °C.	√Blend electrospinning; √Good miscibility between gallic acid and PVA; √Diameters of the electrospun fibers increase with more loaded gallic acid.
Poly(ethylene oxide) (PEO)	Water-soluble and low toxic; Appropriate for co-electrospinning with proteins and charged polysaccharides.	Encapsulation of T4 bacteriophage in electrospun PEO/cellulose diacetate fibers. [93]	Rapid phage release due to hydrophilic polymer shell; Reduced phage release profile for PEO molecular weight.	√Coaxial electrospinning; √Increase of fiber diameter with PEO molecular weight added; √Morphology of post-release fiber: from discontinuous to minimally swollen; √Improvement of potential electrospinning as the change of the physical and electrical conductivity characteristics.
Bioative glass	Excellent bioactivity, osteoconductivity, and osteoinductivity.	Electrospun nanofibers of antibacterial bioactive glass/PEO for wound healing. [94]	Significant cell proliferation (82%) in a period of 24 h; Almost two times of antibacterial activity.	√Blend electrospinning; √Optimum rheological properties: ethanol:water (70:30), bioactive glass (BG) sol: BUTVAR® B-72 solution v/v (3:2).
Polyvinylpyrrolidone (PVP)	Low toxic, hydrophyl, good-adhesion and biocompatible.	Encapsulation ofβ-carotene within electrospun PVP nanofibers. [95]	Maintained the antioxidant activity after the nanoencapsulation.	√Blend electrospinning; √High processable; √The average diameters of PVP/ β-carotene: 176–306 nm; √The average diameter increases with precursor solution increases. But the electrospinning failed at precursor solution of 12 wt.% PVP.
		The anti-bacterial effect of *Aloe vera* acetate-Polyvinylpyrrolidone (AvAc/ PVP) electrospun fibers. [96,97]	The prepared electrospun nanostructures showed great biocompatibility, biodegradability, anti-bacterial and anti-viral activity.	√Blend electrospinning; √The average diameters of the composite fibers increase with the increase of the percentage of Aloe vera, but the fiber became finer with the increase of Aloe vera acetate.
Poly(lactic acid) (PLA)	Biocompatible, non-toxic, linear aliphatic thermoplastic polyester. Biodegradable, and soluble in organic solvents.	Electrospun PLA-chitosan core-shell nanofibers. [98]	Two-stage release behavior of curcumin drug: an initial burst release followed by a sustained release. Encapsulation efficiency (EE) enhanced with the polymers concentration;	√Coaxial electrospinning; √Bead-free smooth fibers with an average diameter of 671 ± 172 nm and a broad diameter distribution.
Poly (ε-caprolactone) (PCL)	Biocompatible aliphatic polyester, low melting point and high decomposition temperature.	Encapsulation of carvacrol within starch or PCL electrospun nanofibers. [99]	Specific bioactive functionality needs to be discussed further.	√Blend electrospinning; √Nanofibers formed mainly with PCL, while beads were obtained with starch systems; √Tightly adhered electrospun layers: highest PCL concentration (15%) and CA ratio (15%).
Natural biopolymers				
Thermoplastic carboxymethyl cellulose (TCMC)	Soluble in a vast variety of solvents, high modulus, adequate flexural, plus good tensile strength.	Drug carriers with electrospun nanostructures of TCMC with PEO. [100]	The nanofibers were non-toxic; Slow and sustained drug release; Excellent bactericidal activity against a wide range of bacteria.	√Coaxial electrospinning. √Fiber morphology: smooth and beadles.
Chitin	Non-toxic, biocompatible, biodegradable polymer with limited solubility, high molecular weight and low chemical reactivity.	Electrospinning ofβ-chitin extracted from cuttlefish bone. [101]	Have great potential as nanomaterials for wound healing.	√Blend electrospinning; √Remarkable increase of electrospinnability when β-chitin was blended with PEO; √The diameter of nanofibers and thickness of the nanofibrous web reduced after the elimination of PEO.
Chitosan (CS)	Biodegradable and biocompatible with antibacterial properties.	Preparation of resveratrol loaded chitosan:gellan (CS:Gel) nanofibers (NFs). [102]	Higher antioxidant activities; Similar cytotoxicity against HT29 cancer cells with compared to free resveratrol.	√Blend electrospinning; √Addition of Gel (0.125 and 0.25% w/v) improved the electrospinning process and the quality of NFs, but more increase had negative effect on

(*continued on next page*)

Table 4 (*continued*)

Polymer type	Polymer features	Applications	Bioactivity of electrospun nanofibers	Manufacturability
Starch	Biocompatible, biodegradable, and mucoadhesive	Electrospun nanofibers of native and anionic corn starch. [103]	Potential as carriers for active components in food and packaging applications.	the spinnability of solutions and morphology of fibers; √The diameter of fibers at 90:10 of CS:Gel solutions was significantly increased to 291 ± 41 nm. √Blend electrospinning √Hard to electrospinning because of its branched amylopectin structures; √Increase of homogeneous and less beaded structures generated by anionic Hylon V; √The fibers are smooth with amylose contents of <70% (w/w).
Pullulan (PUL)	Water soluble, non-toxic, non-immunogenic, non-mutagenic, and noncarcinogenic polymer.	Electrospun chitosan/pullulan nanofibers for drug delivery. [104]	Fast dissolving oral films (FDOFs) exhibit excellent thermal stability and fast solubility.	√Blend electrospinning; √High electrospinnability; √The diameter of nanofibers decreased initially then increased with the increase of chitosan; √Electrospinning process decreased the crystallinity of materials.
Cinnamon Oil	Natural insecticide, volatile.	Antibacterial and antifungal properties and acaricidal effect against house dust mites of core/sheath structured electrospun nanofibers cinnamon oil/PVA. [105]	The antibacterial and antifungal properties, potential acaricidal effect on house dust mites. Continuous release of functional ingredients over 28 days.	√Emulsion electrospinning; √Number of beads increased and diameter increased with increase of the concentration of PVA. √The best conditions for smooth fiber with even fiber size distribution: solution feed rate of 0.2 mL/h, a voltage of 25 kV, and a tip-to-collector distance of 20 cm through a 23-gauge.
Whey protein (WP)	Antioxidant, anti-cancer, antidiabetic, anti-obesity and cardio-protective activities.	Electrospinnability of WP isolate (WPI)/soy protein isolate (SPI) mixed with maltodextrin. [106]	Need to be further discussed.	√Needleless electrospinning; √Spinnability of maltodextrin-soy protein isolate blends was low; √Removal of the insoluble SPI fraction improved spinnability of the spinning dispersion; √Protein content was linked to the spinnability and fiber appearance.

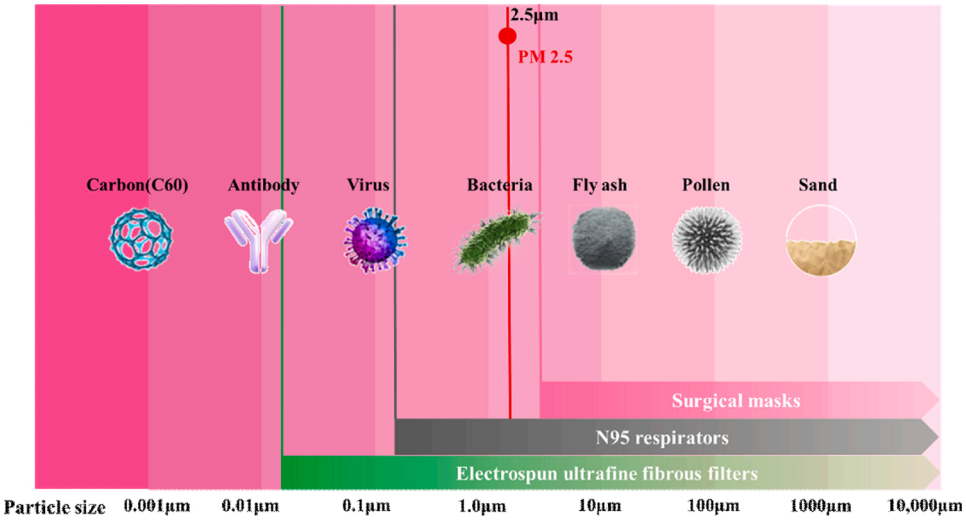

Fig. 6. The comparison of filtration performance of electrospun ultrafine fibrous filters, N95 respirators and commonly used surgical facemasks.

(TPU), which is able to remove PM 2.5 with the filtration efficiency of 99.654% and good optical transparency of 60%. The removal efficiency is only reduced by 1.6% after 10 times of filtration [115](Fig. 7a). Lee et al. developed an electrospun polybenzimidazole (PBI) nanofiber membrane with high $PM_{2.5}$ filtering efficiency of ~98.5% at a much-reduced pressure drop of 130 Pa [116]. This PBI filter showed thermal stability after applying thermal stress on a hot plate at 400 °C for 1 h and retained its original performance after several cycles of cleaning (Fig. 7b, c). Moreover, the O_2 Nano Mask was recently created successfully by Viaex Technologies [117]. This mask is composed of reusable skin and replaceable filter, in which the diameters of fibers are between 85 ± 20 nm. The O_2 Nano Mask achieved 99% particle removal efficiency and was machine washable.

Besides, some researchers developed reusable and self-powered

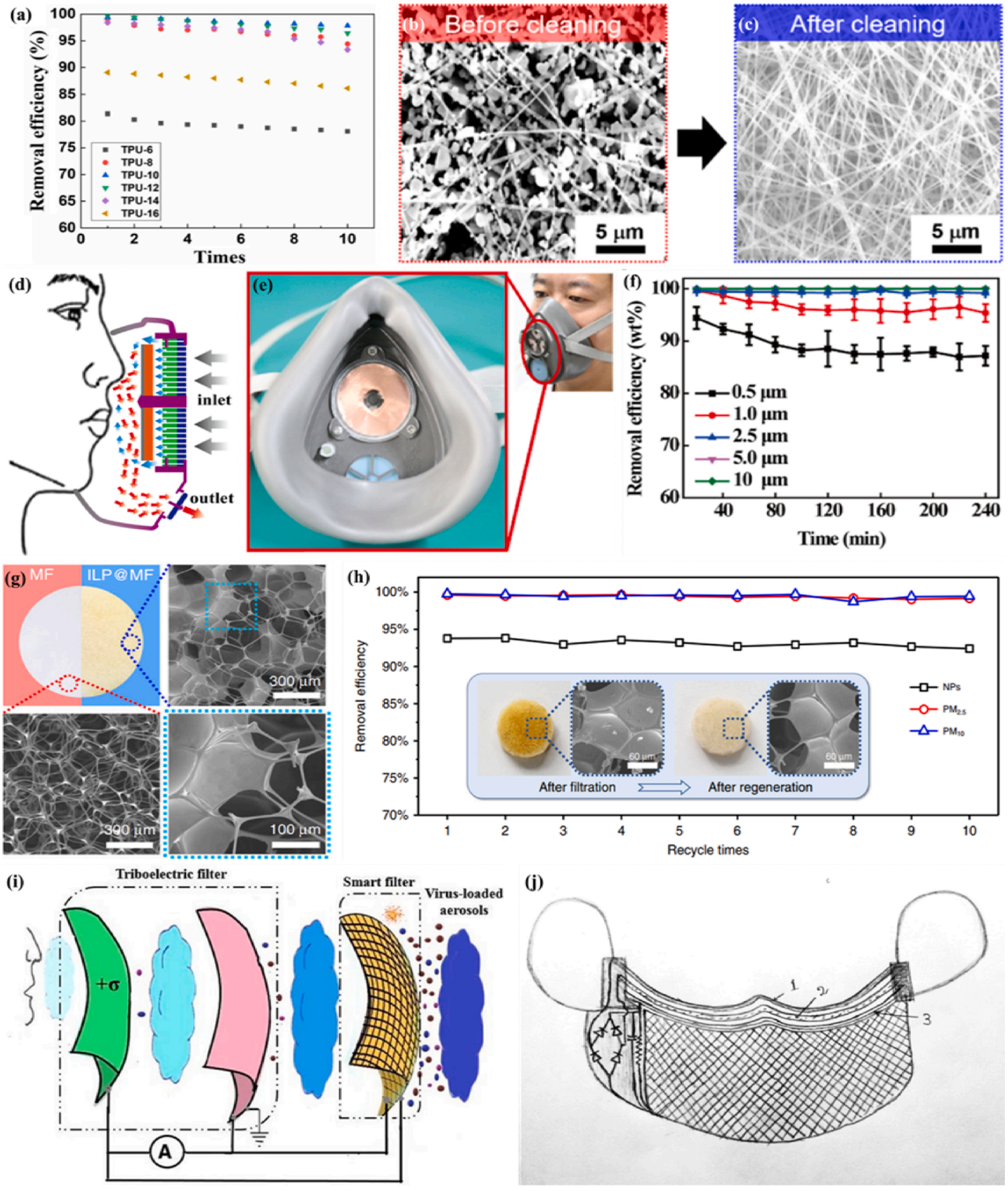

Fig. 7. (a) Reusability of the TPU-10 nanofiber filter. Reproduced with permission from [115]. Copyright 2019, Nanoscale Research Letters. (b) and (c) SEM images showing nanofibers of the PBI filter before and after the cleaning process using inorganic particulate matters. Reproduced with permission from [116]. Copyright 2019, ACS Applied Materials and Interfaces. (d) Structure of the R-TENG. (e) Digital photo of the SEA-FM. (f) Durability test on the removal efficiency of the SEA-FM after 30 days. Reproduced with permission from [118]. Copyright 2018, ACS Applied Materials and Interfaces. (g) Photographs and SEM images of the MF sponge (red) and the ILP@MF filter (blue). (h) Filtration efficiency of the charged [C_4mim][OAc]–PVP@MF filter regenerated for 1–10 times. Reproduced with permission from [119]. Copyright 2020, Nature Communications. (i) The schematic of the working mechanism of self-powered smart masks. (j) The proposed self-powered smart mask (1-inner layer, 2-middle layer, 3-smart layer). Reproduced with permission from [120]. Copyright 2020, arXiv:2005.08305. (For interpretation of the references to colour in this figure legend, the reader is referred to the web version of this article).

masks by utilizing wearable technology. For example, Liu et al. developed a novel self-powered electrostatic adsorption face mask (SEA-FM) based on the poly(vinylidene fluoride) electrospun nanofiber film (PVDF-ESNF) and a triboelectric nanogenerator (TENG) driven by respiration (R-TENG) (Fig. 7d,e) [118]. It showed that the removal efficiency of coarse and fine particulates was higher than 99.2%, and the removal efficiency of ultrafine particulates was as high as 86.9% after continually wearing for 240 min (Fig. 7f). Zhang et al. developed a self-powered ILP@MF air filter (Fig. 7g) based on ILP composites (metal/halogen-free IL 1-alkyl-3-methylimidazolium acetate and hydrophilic polymers, including poly(acrylamide) (PAM), poly(vinyl alcohol) (PVA) and poly(vinylpyrrolidone) (PVP)) and melamine-formaldehyde (MF), which achieved removal for nanoparticles with an efficiency of 93.77% [119]. In this study, a power source (micro-button lithium cell or silicon-based solar panel) is employed as a power supply platform, which enable the reusability while maintaining high efficiency (Fig. 7h). Recently, Ghatak et al. designed a self-powered smart face mask for the filtration of SARS-CoV-2 in combination with textile fibers [120]. The smart mask was composed of multilayer protection sheets, in which the first two layers acted as a triboelectric (TE) filter while the outer layer was a smart filter (Fig. 7i, j). It achieved destroying the viral particles through double action of charge adsorption and electrocution by triboelectrification. Moreover, this smart face mask was reusable due to the self-driven mechanism, which harvested mechanical energy from breathing, talking, or other facial movement functionalities. In the future, the modified attempt toward enhancing the filtering performance may try to introduce electrospun ultrafine fibers.

4.5. Potential in protective devices

The electrospun ultrafine fibers, serving as ideal protective devices [121,122], have shown great capabilities to protect against nanoparticulate aerosols, chemicals like nerve agents, mustard gas, and

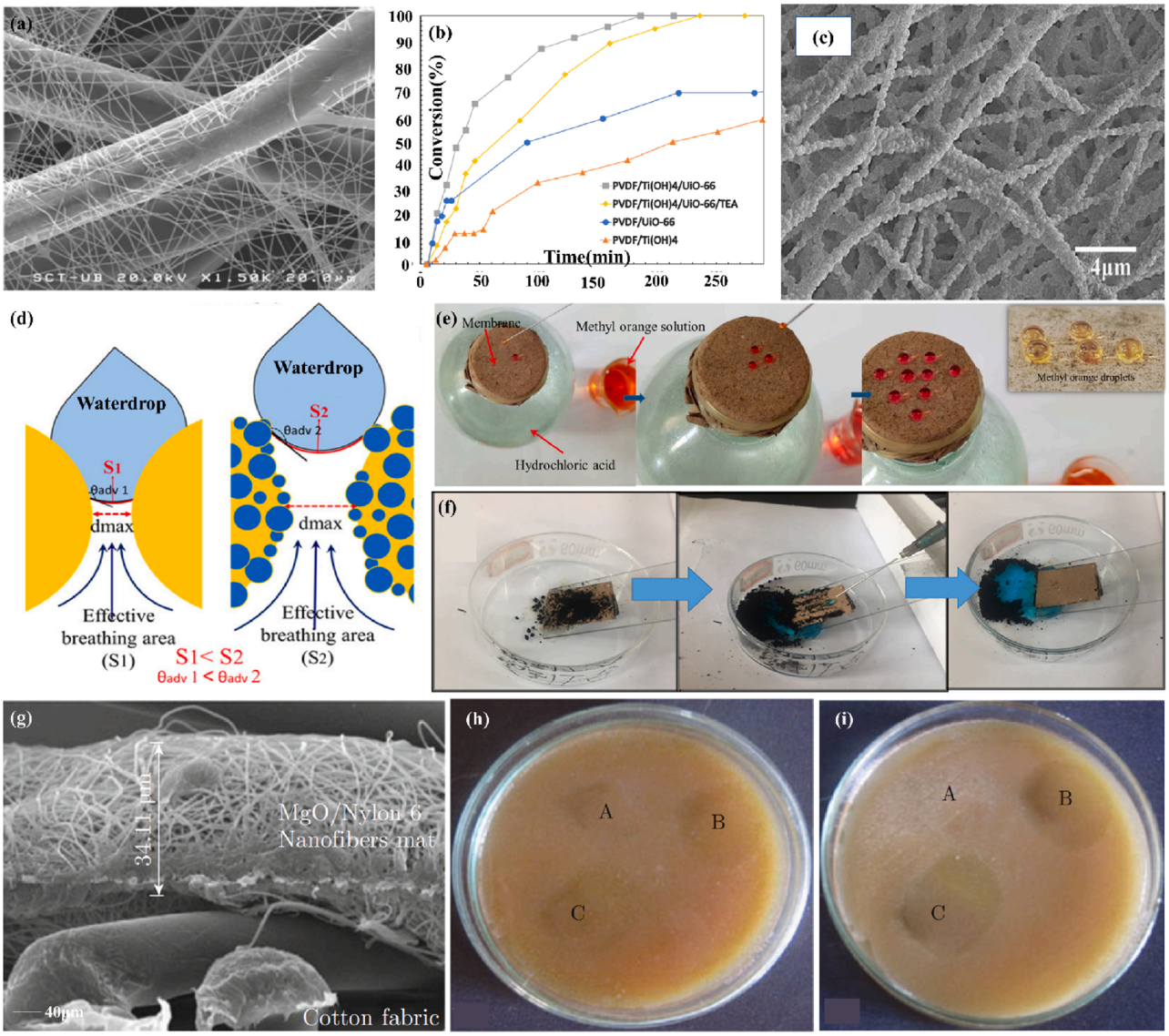

Fig. 8. (a) SEM image of PA6 electrospun nanofibers that thermally bonded onto the viscose non-woven. Reproduced with permission from [123]. Copyright 2012, Journal of Nanomaterials. (b)The percent conversion of GD nerve agent with PVDF composite samples. Reproduced with permission from [124]. Copyright 2018, ACS Applied Materials & Interfaces. (c) SEM image of 7.3 wt% SiO_2@PTFE. (d) Schematic illustration of porous structure and breathability of BLNFMs. (e) Breathable performance of BLNFMs. (f) Self-cleaning performance of the superhydrophobic BLNFMs. Reproduced with permission from [126]. Copyright 2018, Applied Surface Science. (f) FE-SEM image show the cross section view of MN6C. Antibacterial activities of (g) *Staphylococcus aureus* and (h) *Escherichia coli*. A-UC, B-N6C, and C-MN6C. Reproduced with permission from [128]. Copyright 2014, Nano-Micro Letters.

biological threats including bacterial spores, viruses, etc. In one study, efficient protective clothing against nanoparticulate aerosols was fabricated by depositing nanofibrous mats of polyamide 6 (PA6) onto a nonwoven viscose substrate with a PA6 fiber diameter ranging from 66 to 195 nm [123](Fig. 8a). The nanofiber layer thickness strongly desired the penetration of NaCl particles with a diameter ranging from 15 to 300 nm; it provided up to 80% retention of 20 nm size particles and over 50% retention of 200 nm size nanoparticles. Dwyer et al. fabricated chemical protective clothing against GD nerve agent with high filtration efficiency by incorporating UiO-66, a zirconium-based metal-organic framework (MOF), into PVDF/Ti$(OH)_4$ composite fabric [124] (Fig. 8b). In this study, it had 100% filtration efficiency with particles ranging from 0.05−0.40 μm in diameter for PVDF/Ti$(OH)_4$ and PVDF/Ti $(OH)_4$/UiO-66.

Waterproof and breathable (W&B) clothing can not only protect the wearer from external harmful liquids but also provide a good level of comfort [125]. Liang et al. fabricated super-hydrophobic self-cleaning bead-like SiO_2@PTFE nanofiber membranes with the modest vapor permeability of 9.7 kg m^{-2} D^{-1} and air permeability of 7.2 mm s^{-1}. It showed the potential waterproof/breathable applications in real environments with self-cleaning protection [126] (Fig. 8c-f). Kharaghani et al. fabricated a washable nanofiber membrane with high-dispersed silver nanoparticles to form the hierarchically organized antibacterial breath mask by designing and synthesizing polyacrylonitrile/silver nanoparticles (PAN/AgNPs) nanofibers via an *in-situ* method [127]. The antibacterial ability after washing was directly related to the release

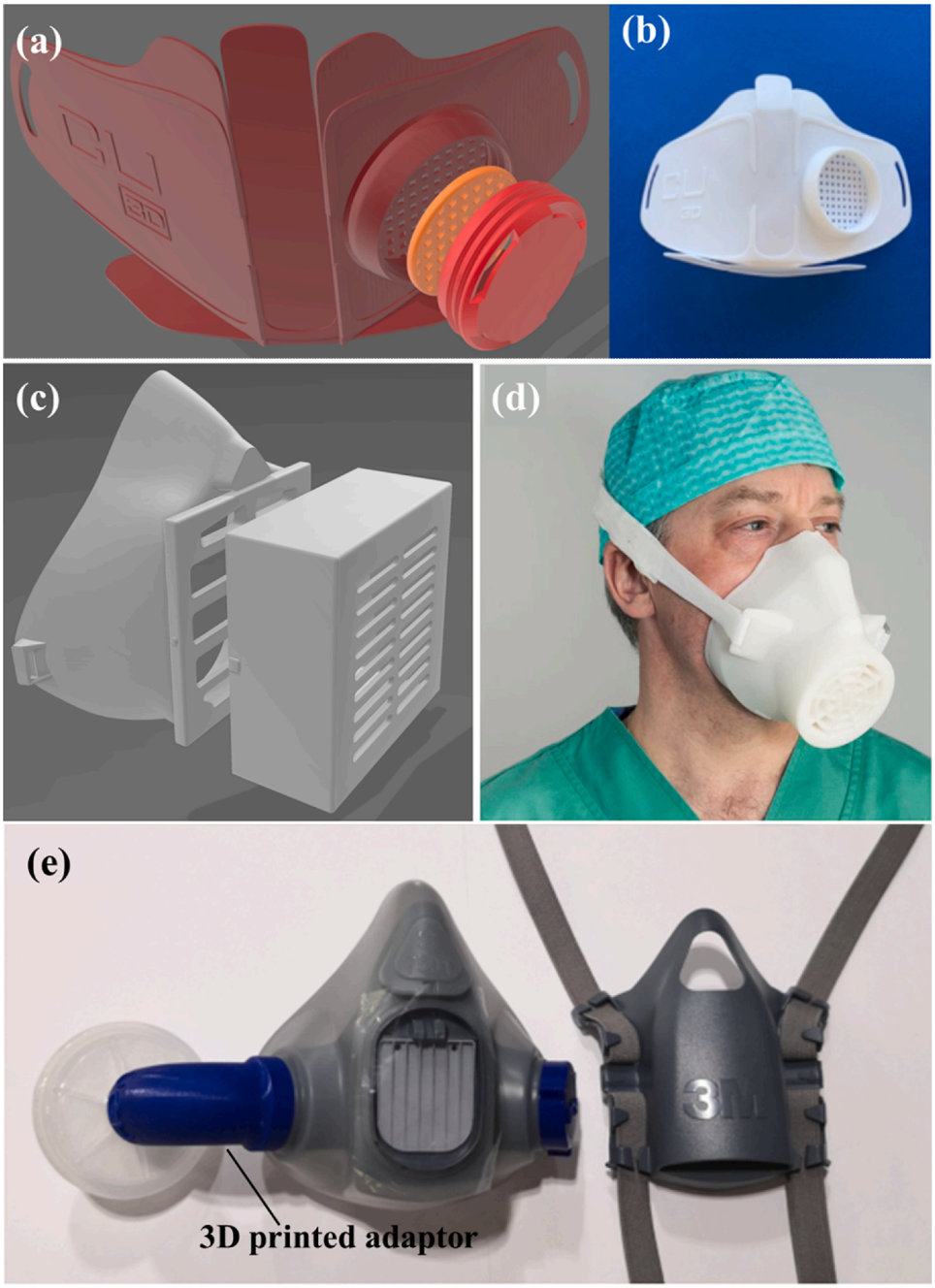

Fig. 9. (a, b) Copper3D NanoHack mask. (c,d) HEPA mask design with a box for filter insertion. Reproduced with permission from [135]. Copyright 2020, International Journal of Oral and Maxillofacial Surgery. (e) The 3D-printed adaptor on reusable elastomeric respirators. Reproduced with permission from [136]. Copyright 2020, Anaesthesia.

ability of AgNPs from nanofibers.

Electrospun ultrafine fibers also have wide applications in protecting against bioaerosols like bacteria [129]. Dhineshbabu et al. made a MgO/nylon 6 hybrid nanofiber mat for protective clothing with better fire retardancy and antibacterial activity than those of nylon 6 nanofiber [128] (Fig. 8e-i). In a timely study, Tremiliosi et al. demonstrated the antiviral effectiveness of Ag-based polycotton fabrics against SARS-CoV-2, decreasing the number of replicates by 99.99% after an incubation period of 2 min [23]. It also inhibited 99.99% of the pathogens *S. aureus*, *E. coli,* and *C. Albicans*. This work provides feasible inspiration for the development of antiviral electrospun ultrafine fibrous face masks.

5. Innovations of face masks

5.1. 3D-printed masks/respirators with replaceable filters

The 3D-printed masks with replaceable nanofiber filter inserts have caused great attention for the reusability, user comfort and protective performance. Recently, a 3D printed face mask named Copper3D NanoHack (Fig. 9a, b) [130] was developed through 3D printing PLA as the mono-block structure and TPU based material as the outer rim. The mask includes a simple air intake port with two reusable filters inserted, using a screw-in cover to hold the filters [131]. The purpose of using the replaceable nanofiber filter is to offer a degree of protection against airborne particles and to prevent the spread of liquid aerosols that could contaminate the airways. Kvatthro et al. manufactured 3D printed HEPA mask (Fig. 9c) [132] based on PLA filament via desktop printers to ensure the best seal in field conditions. The mask allows space for an exchangeable filter inserts within a port at the front of the mask. An optimized variant of 3D printed mask called the Lowell Makes mask [133] with a replaceable front filter without support or adhesion was developed. This mask may improve user comfort with the addition of foam padding on the inside. Other similar creative work including the flexible mask Valvy [134] on a cloth bed platform, which allows for reusability with dedicated filter inserts.

Furthermore, several efforts especially focusing on medical-grade 3D-printed respirators have also been taken, attempting to get a potential solution for the healthcare professionals. Swennen et al. manufactured 3D-printed face masks for clinic use (Fig. 9d) [135]. However, some essential issues, including the fitting, disinfection process and reusable property, should be investigated in the future. Liu et al. obtained re-usable elastomeric respirators by designing a 3D-printed adaptor that permits the elastomeric interface (Fig. 9e) [136]. This 3D-printed adaptor used in re-usable elastomeric respirators may be a potential alternative to address N95 shortages during the COVID-19 pandemic. In the future, the replaceable nanofiber filter inserts may improve the protective performance, enhance the reusability, and increase the user comfort of the 3D printed face mask.

5.2. Transparent mask

There is a communication barrier between the doctor and the deaf-mute patient when wearing a mask. The filter with high optical transparency can be used for personal protection while making lip-reading available. Besides, it is also viable for decoration engineering. However, there are challenges in making a transparent mask and maintaining its filtration efficiency. In one study, patterned nanofiber air filters with high optical transparency and effective $PM_{2.5}$ capture capability were fabricated via electrospinning technology (Fig. 10b) [137]. The patterned nanofibers exhibited high porosity (>80%) and high $PM_{2.5}$ filtration efficiency of 99.99% with good transmittance of about 69%. Liu et al. designed a novel reusable bilayer fibrous filter consisting of electrospun poly(methylmethacrylate)/polydimethylsiloxane. The unique structure of nanofibers allows it to show a particulate matter (PM) filtration efficiency of over 96% with high optical transmittance of

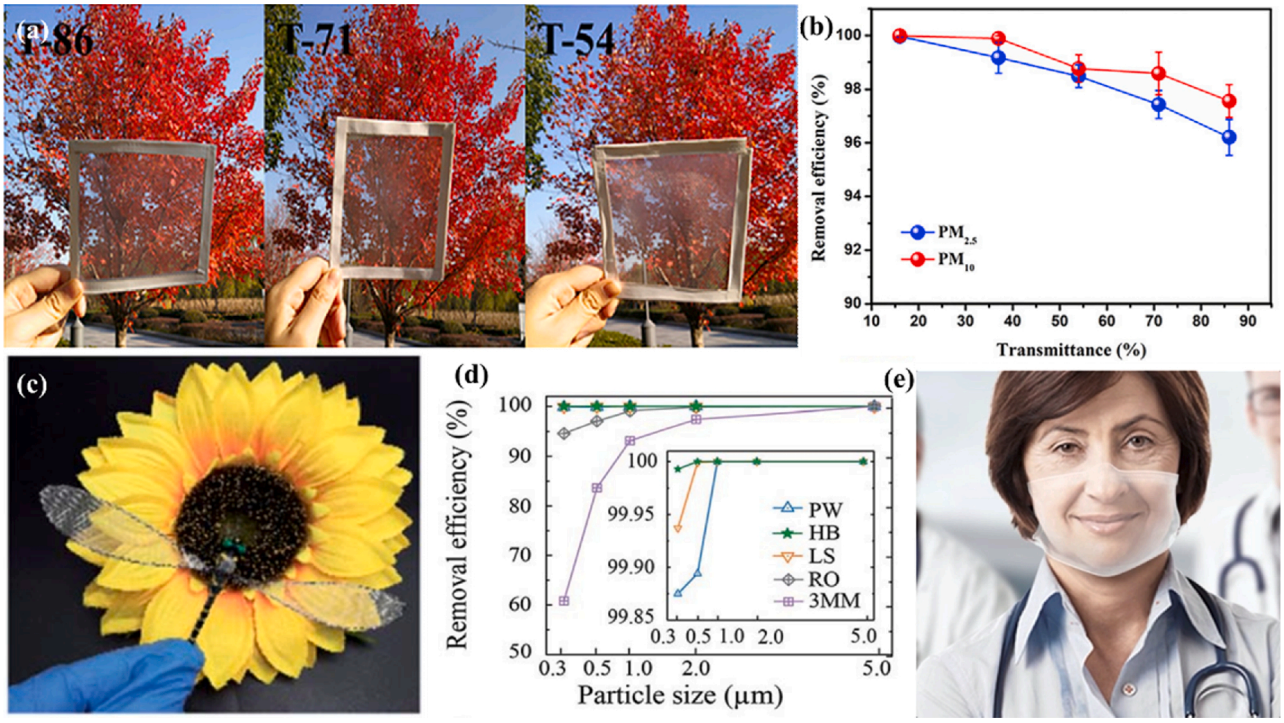

Fig. 10. (a) Photographs of PDMS/PMMA-chitosan transparent air filter with different optical transmittance. (b) PM 2.5 and PM 10 removal efficiency of transparent filters with different transmittances. Reproduced with permission from [138]. Copyright 2019, iScience. (c) The prepared transparent air filter was integrated into the wing of a dragonfly model to observe its transmittance in front of a cloth sunflower. (d) Comparison of the removal efficiency between plain weave (PW), herringbone (HB), lozenge stria (LS) pattern of the fibrous membranes. Reproduced with permission from [137]. Copyright 2020, RSC Advances. (e) The transparent Hello Mask. Reproduced with permission from [140]. Copyright 2020, https://www.empa.ch/web/s604/schutzmaske.

86% (Fig. 10a) [138]. This transparent nano-filter is also reusable with the ability to retain a high PM removal efficiency ($PM_{2.5}$ > 98.39%) after five washing cycles. Recently, He et al. fabricated a biodegradable mask filter with a hierarchical structure and transparent look by printing polylactic acid (PLA) polymer struts on a PLA nanofiber web through electrospinning and 3D printing [139]. Furthermore, researchers from Empa and EPFL are currently developing novel medical masks named Hello Mask (Fig. 10c) [140] with an integrated transparent and biodegradable filter film using electrospinning. This transparent protective mask contains fine membranes with a pore size of around 100 nanometers, which provides effective protection against viruses. At the same time, it eliminated the communication barriers between deaf-mute patients and medical staff.

5.3. Biodegradable masks

The current masks, that are made of non-renewable resources and are non-biodegradable, may create harmful microplastics upon disposal after their single-use, which is pernicious towards the environment [141]. It is considerated to develop masks with biodegradable materials to reduce environmental concerns for a sustainable future in the long run. In one study, biodegradable electrospun poly(l-lactic acid) (PLLA) fibrous filters with high filtering efficiency of 99.3% for $PM_{2.5}$ particles were manufactured [142]. The electrostatic force generated from the electrospun PLLA nanofibers contributes absorption for the submicron particle. Zhang et al. prepared reusable and biodegradable electrospun nanofibrous poly(vinyl alcohol)/cellulose nanocrystals air filter for PM removal (Fig. 11a, b) [143]. This filter can be water washing over 5 cycles while maintaining the $PM_{2.5}$ removal efficiency above 95% and pressure drop less than 100 Pa. Recently, Das et al. proposed fully bio-based facemasks via electrospinning gluten biopolymer into nanofiber membranes to form nanofiber filter media (Fig. 11c) [144]. This mask could be effective in reducing the transmittance of infectious diseases and achieve rapid degradation in outdoor habitats into harmless products promoting the utilization of renewable raw materials.

5.4. The nostril filters

The use of nostril filters is another innovative option to avoid exposure to airborne allergenic particles. The nasal filters placed within the nasal passages are supposed to prevent airborne particles from entering the respiratory system. The conventional nasal filters are made of woven nontoxic mesh, non-woven type, or porous filters. It could reduce daily sneezing times and runny nose by an average 45% and 12%, respectively [145]. Nanotechnology enabled nasal filters can be more effective to catch nanoparticles before entering into the host and also offer additional features such as flexibility and minimum pressure drop [146]. Han et al. designed a novel nanofiber nasal filter (NNF) by overlaying a carbon filter substrate with electrospun nylon nanofibers (Fig. 12a, b) [147]. The filters can achieve filtering efficiency more than 90% for particles > 1 μm and 50% efficiency for particles < 0.5 μm without significant pressure drop, which is about 2.3-fold improvement compared to commercially available nasal filters. The filters have great potential in personal protective equipment against exposure to ultrafine particles. Srikrishnarka et al. fabricated an enhanced protective electrospun nanofiber filter mat consisting of chemically treated electrospun PAN and PS fibers, with which can capture $PM_{0.3}$ with efficiency of ~93% and maximum pressure drop across the fibers being < 60 Pa [148]. Furthermore, the breathing comfort of filter placed inside a silicone-based nasal plug was tested, which demonstrated the potential in nasal plugs for personal protection. Nevertheless, the nostril filters may cause secondary infection when used for blocking viruses.

6. Conclusions and outlook

In summary, the unprecedented swift spread of the COVID-19 caused by SARS-CoV-2 has caused global public health concern. Wearing a mask is an important means to slow down the spread of the virus. However, the currently commercial masks are designed to be used within several hours and disposal, leading to a critical worldwide shortage. This article first introduces the basic knowledge of SARS-CoV-2 and other viruses. Ultrafine fibers are highly regarded in air filtration applications due to their high surface area and small inter-fiber pore

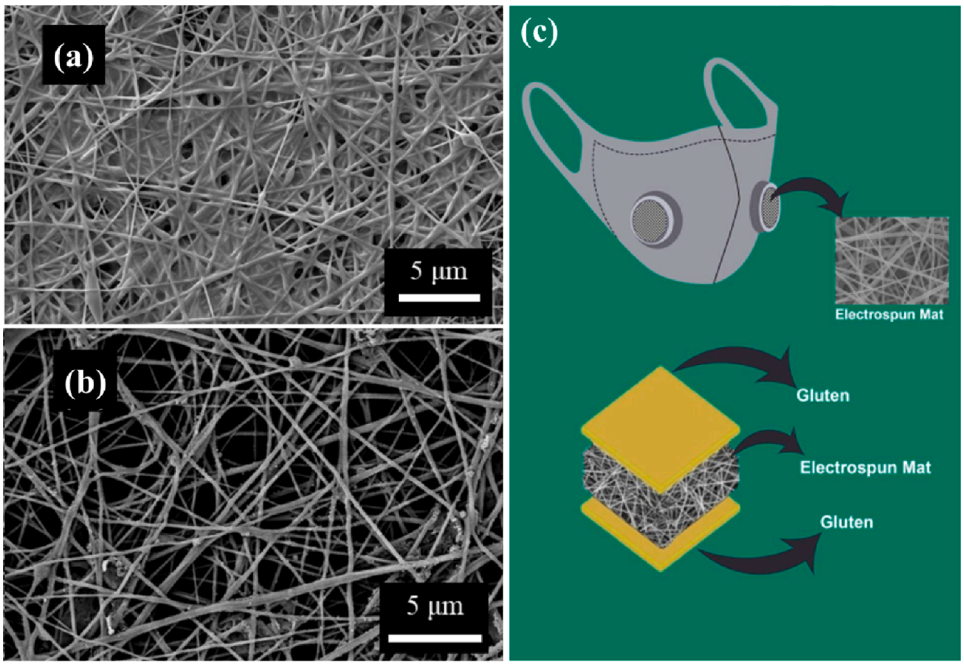

Fig. 11. SEM images of fouled PVA/CNCs filters (a) before (b) after water washing. Reproduced with permission from [143]. Copyright 2020, Chemical Engineering Journal. (c) Schematic showing the final shape and internal structure of the fully bio-based facemasks. Reproduced with permission from [144]. Copyright 2020, Science of the Total Environment.

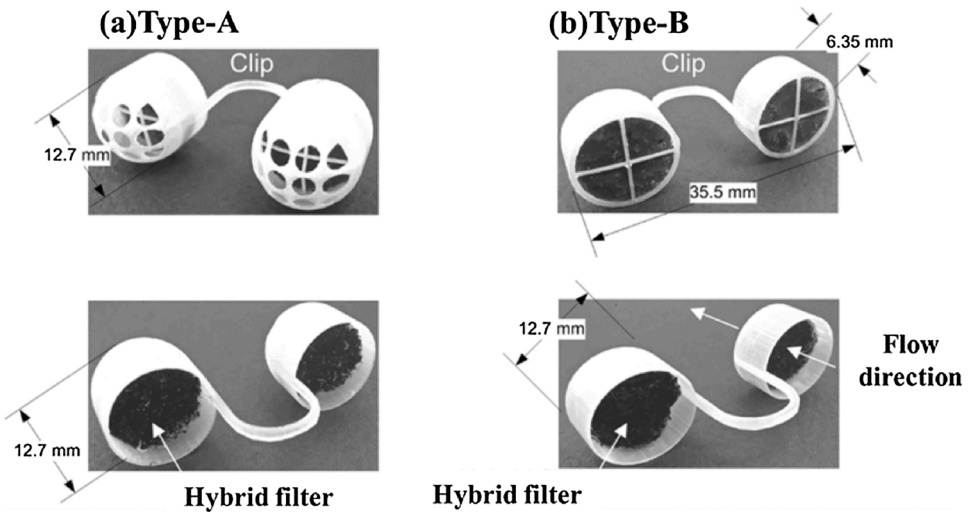

Fig. 12. Photos of the prototypes of NNF (a) type-A and (b) type-B: the frames fabricated by using a 3D printer and then a pair of hybrid filters were installed. Reproduced with permission from [147]. Copyright 2018, Aerosol and Air Quality Research.

size. We highlighted Electrospinning as one of the most versatile and viable techniques for generating ultrafine fibers. Electrospun ultrafine fibrous filters have shown high filtering efficiency of fine particles and aerosols. Furthermore, the electrospun ultrafine fibrous filters have great potential in reusable applications and personal protective devices by incorporating appropriate fibers/polymers with functional materials. Significantly, researchers are recently making great efforts to innovatively develop 3D-printed respirators, transparent and biodegradable masks, and nostril filters, responding to COVID-19. They may also be involved in future innovations toward masks.

The development of advanced masks/respirators will play a crucial role in protecting against epidemic like COVID-19. The advanced masks, including the reusable masks, antiviral masks, and biodegradable masks, have shown exciting benefits. Whereas the related standards for their design and test are few, which may possibly confuse the public to a certain extent. Meanwhile, the commercial industrializations of certain advanced masks/respirators may not be available due to the undoubtedly increasingly enormous research and development cost. In the future, the development of the relevant policies and standards will be beneficial to the improvement of advanced masks/respirators. The key to lower the cost and design the functionality of advanced masks is still lying in materials advances, which will also determine the whole industrial developmental sustainability. The research of electrospun ultrafine fibrous filters for advanced masks/respirators will be greatly promising in this area.

Author contributions

ZFZ and DXJ wrote the paper, DXJ and SR planned the content of the article. All authors read and approved the final manuscript.

Declaration of Competing Interest

The authors declare no conflict of interest.

Acknowledgements

This work was supported by the NUS COVID-19 Research Seed Funding (Reference No: NUSCOVID19RG-11).

References

[1] C.S.G. of the International, Nat. Microbiol. 5 (2020) 536–544.
[2] M. Xie, Q. Chen, Int. J. Infect. Dis. 94 (2020) 119–124.
[3] H.A. Rothan, S.N. Byrareddy, J. Autoimmun. 109 (2020) 102433–102437.
[4] Y.-Y. Zheng, Y.-T. Ma, J.-Y. Zhang, X. Xie, Nat. Rev. Cardiol. 17 (2020) 259–260.
[5] C. Huang, Y. Wang, X. Li, L. Ren, J. Zhao, Y. Hu, L. Zhang, G. Fan, J. Xu, X. Gu, Lancet 395 (2020) 497–506.
[6] S. Feng, C. Shen, N. Xia, W. Song, M. Fan, B.J. Cowling, Lancet Respir. Med. 8 (2020) 434–436.
[7] Y. Bai, L. Yao, T. Wei, F. Tian, D.-Y. Jin, L. Chen, M. Wang, Jama 323 (2020) 1406–1407.
[8] B. Cowling, Y. Zhou, D. Ip, G. Leung, A. Aiello, Epidemiol. Infect. 138 (2010) 449–456.
[9] W.H. Organization, Newsroom, March 3 (2020), 2020.
[10] D. Ji, L. Fan, X. Li, S. Ramakrishna, BMC Mater. 2 (2020) 1–11.
[11] Z. Zhang, H. He, W. Fu, D. Ji, S. Ramakrishna, Nano Today 35 (2020), 100942.
[12] A. Poudyal, G.W. Beckermann, N.A. Chand, I.C. Hosie, A. Blake, B. Kannan, Electrospun Nanofibre Filter Media: New Emergent Technologies and Market Perspectives, Filtering Media by Electrospinning, Springer, 2018, pp. 197–224.
[13] L. Weng, J. Xie, Curr. Pharm. Des. 21 (2015) 1944–1959.
[14] R. Gahan, G.C. Zguris, A Review of the Melt Blown Process, Fifteenth Annual Battery Conference on Applications and Advances (Cat. No. 00TH8490), IEEE, 2000, pp. 145–149.
[15] G. Borkow, S.S. Zhou, T. Page, J. Gabbay, PLoS One 5 (2010), e11295.
[16] N.J. Dimmock, A.J. Easton, K.N. Leppard, Introduction to Modern Virology, John Wiley & Sons, 2016.
[17] I.O.f. Standarzation, ISO 18184-2019:Textiles-Determination of Antiviral Activity of Textile Products, British, 2019, pp. 1–50.
[18] A. Isaacs, J. Lindenmann, Proc. Roy. Soc. Lond. Series B-Biol. Sci. 147 (1957) 258–267.
[19] M.G. Rossmann, J.E. Johnson, Annu. Rev. Biochem. 58 (1989) 533–569.
[20] A. Czeglédi, D. Ujvári, E. Somogyi, E. Wehmann, O. Werner, B. Lomniczi, Virus Res. 120 (2006) 36–48.
[21] M.A. Brinton, Ann. N. Y. Acad. Sci. 951 (2001) 207–219.
[22] R. Sender, S. Fuchs, R. Milo, PLoS Biol. 14 (2016), e1002533.
[23] G.C. Tremiliosi, L.G.P. Simoes, D.T. Minozzi, R.I. Santos, D.B. Vilela, E.L. Durigon, R.R.G. Machado, D.S. Medina, L.K. Ribeiro, I.L.V. Rosa, BioRxiv (2020).
[24] M. Lipsitch, S. Siller, M.A. Nowak, Evolution 50 (1996) 1729–1741.
[25] A.R. Lohe, E.N. Moriyama, D.-A. Lidholm, D.L. Hartl, Mol. Biol. Evol. 12 (1995) 62–72.
[26] R. Tellier, J. R. Soc. Interface 6 (2009) S783–S790.
[27] F.M. Burnet, Arch. Intern. Med. (1945) 495.
[28] B. S, Introduction to Modern Virology, Blackwell Science, 1994.
[29] A.C. Walls, Y.-J. Park, M.A. Tortorici, A. Wall, A.T. McGuire, D. Veesler, Cell 181 (2020) 281–292.
[30] N. Zhu, D. Zhang, W. Wang, X. Li, B. Yang, J. Song, X. Zhao, B. Huang, W. Shi, R. Lu, N. Engl. J. Med. 382 (2020) 727–733.
[31] M.A. Tortorici, D. Veesler, Structural Insights into Coronavirus Entry, Advances in Virus Research, vol 105, Elsevier, 2019, pp. 93–116.
[32] Z. Wu, J.M. McGoogan, JAMA 323 (2020) 1239–1242.
[33] L. Ferretti, C. Wymant, M. Kendall, L. Zhao, A. Nurtay, L. Abeler-Dörner, M. Parker, D. Bonsall, C. Fraser, Science 368 (2020) eabb6936–eabb6948.
[34] L. Setti, F. Passarini, G. De Gennaro, P. Barbieri, M.G. Perrone, M. Borelli, J. Palmisani, A. Di Gilio, P. Piscitelli, A. Miani, Airborne Transmission Route of COVID-19: Why 2 meters/6 Feet of Inter-personal Distance Could Not Be Enough, Multidisciplinary Digital Publishing Institute, 2020.
[35] L. Morawska, J. Cao, Environ. Int. (2020), 105730.
[36] M. Doucleff, Ebola In The Air: What Science Says About How The Virus Spreads, HEALTH, 2014. https://www.npr.org/sections/goatsandsoda/2014/12/01/364749313/ebola-in-the-air-what-science-says-about-how-the-virus-spreads.

[37] H.A. Aboubakr, T.A. Sharafeldin, S.M. Goyal, Transboundary and Emerging Diseases, 2020.
[38] N. Van Doremalen, T. Bushmaker, D.H. Morris, M.G. Holbrook, A. Gamble, B. N. Williamson, A. Tamin, J.L. Harcourt, N.J. Thornburg, S.I. Gerber, N. Engl. J. Med. 382 (2020) 1564–1567.
[39] A. Chin, J. Chu, M. Perera, K. Hui, H.-L. Yen, M. Chan, M. Peiris, L. Poon, medRxiv (2020).
[40] K.-H. Chan, S. Sridhar, R.R. Zhang, H. Chu, A.-F. Fung, G. Chan, J.-W. Chan, K.-W. To, I.-N. Hung, V.-C. Cheng, J. Hosp. Infect. 106 (2020) 226–231.
[41] A. Kratzel, S. Steiner, D. Todt, P. V'kovski, Y. Brueggemann, J. Steinmann, E. Steinmann, V. Thiel, S. Pfaender, J. Infect. 81 (2020) 452–482.
[42] J. Wu, F. Xu, W. Zhou, D.R. Feikin, C.-Y. Lin, X. He, Z. Zhu, W. Liang, D.P. Chin, A. Schuchat, Emerging Infect. Dis. 10 (2004) 210–219.
[43] D.S. Hui, B.K. Chow, L. Chu, S.S. Ng, N. Lee, T. Gin, M.T. Chan, PLoS One 7 (2012) e50845–e50853.
[44] SARS-CoV-2, 2020.
[45] C.K. Brown, Health Secur. 17 (2019) 133–139.
[46] M. Ippolito, F. Vitale, G. Accurso, P. Iozzo, C. Gregoretti, A. Giarratano, A. Cortegiani, Pulmonology 26 (2020) 204–212.
[47] Cf.D. Control, Prevention, MMWR. Morbidity and Mortality Weekly Report, vol. 47, 1998, pp. 1045–1049.
[48] J. Santos, C. Varela, Thecnical document. Stockholm: European Centre for Disease Prevention and Control (ECDC), ECDC, 2014.
[49] T. Cook, Anaesthesia, 2020, pp. 920–927.
[50] W.H. Organization, Advice on the Use of Masks in the Context of COVID-19: Interim Guidance, 5 June 2020, World Health Organization, 2020.
[51] A. Repici, R. Maselli, M. Colombo, R. Gabbiadini, M. Spadaccini, A. Anderloni, S. Carrara, A. Fugazza, M. Di Leo, P.A. Galtieri, Gastrointest. Endosc. (2020) 192–197.
[52] FDA, Premarket Notification 510(k), 2020.
[53] H. Delaney, R. Van de Zande, A Guide to EU Standards and Conformity Assessment, 2000.
[54] FDA, Device Registration and Listing, 2020.
[55] C.f.D.a.R. Health, (2020).
[56] D.R. Challoner, U. Senate, Medical Devices and the Public's Health: the FDA 510 (k) Clearance Process at 35 Years, Written Statement Before the Committee on Health, Education, Labor, and Pensions US Senate, Institute of Medicine of the National Academics, Washington, 2011.
[57] C.f.D.a.R. Health, Enforcement Policy for Face Masks and Respirators During the Coronavirus Disease (COVID-19) Public Health Emergency (Revised), United Stateds, 2020.
[58] FDA, FDA Webinar Series- FDA's Regulation of Face Masks and Surgical Masks During the COVID-19 Pandemic, 2020.
[59] C.f.D.a.R.H.C.f.B.E.a, Research, The Abbreviated 510(k) Program, 2019.
[60] S. Rengasamy, R. Shaffer, B. Williams, S. Smit, J. Occup. Environ. Hyg. 14 (2017) 92–103.
[61] FDA, Personal Protective Equipment EUAs, 2020.
[62] C.-C. Chen, K. Willeke, Am. J. Infect. Control 20 (1992) 177–184.
[63] Z. Feng, S.-J. Cao, Sustain. Cities Soc. 49 (2019) 101569–101580.
[64] S. Ullah, A. Ullah, J. Lee, Y. Jeong, M. Hashmi, C. Zhu, K.I. Joo, H.J. Cha, I.-S. Kim, ACS Appl. Nano Mater. 3 (2020) 7231–7241.
[65] N.P.B. Tan, S.S. Paclijan, H.N.M. Ali, C.M.J.S. Hallazgo, C.J.F. Lopez, Y.C. Ebora, ACS Appl. Nano Mater. 2 (2019) 2475–2483.
[66] H.Y. Chung, Book Review, Electrospinning of Micro-and Nanofibers: Fundamentals in Separation and Filtration Processes, SAGE Publications Sage UK, London, England, 2008.
[67] A. Mukhopadhyay, Text. Prog. 42 (2010) 1–97.
[68] F.J. Romay, B.Y. Liu, S.-J. Chae, Aerosol Sci. Technol. 28 (1998) 224–234.
[69] Z. Feng, Z. Long, T. Yu, J. Electrostat. 83 (2016) 52–62.
[70] A. Kilic, E. Shim, B.Y. Yeom, B. Pourdeyhimi, J. Electrostat. 71 (2013) 41–47.
[71] P.P. Tsai, H. Schreuder-Gibson, P. Gibson, J. Electrostat. 54 (2002) 333–341.
[72] R.H. Bamberger, M.J. Smith, Ieee Trans. Signal Process. 40 (1992) 882–893.
[73] N. Hiremath, G. Bhat, Nanosci. Technol. 2 (2015) 1–9.
[74] Y. Zhang, S. Yuan, X. Feng, H. Li, J. Zhou, B. Wang, J. Am. Chem. Soc. 138 (2016) 5785–5788.
[75] S. Ramakrishna, K. Fujihara, W.-E. Teo, T. Yong, Z. Ma, R. Ramaseshan, Mater. Today 9 (2006) 40–50.
[76] X. Li, Y. Gong, J. Chem. 2015 (2015) 460392–460397.
[77] Y. Li, K. Xiao, J. Luo, J. Lee, S. Pan, K.S. Lam, J. Control. Release 144 (2010) 314–323.
[78] T. Grafe, K. Graham, Int. Nonwovens J. (2003), 1558925003os-1551200113.
[79] J. Xue, T. Wu, Y. Dai, Y. Xia, Chem. Rev. 119 (2019) 5298–5415.
[80] Z.M. Huang, C.L. He, A. Yang, Y. Zhang, X.J. Han, J. Yin, Q. Wu, J. Biomed. Mater. Res. A 77 (2006) 169–179.
[81] M. Tebyetekerwa, Z. Xu, S. Yang, S. Ramakrishna, Adv. Fiber Mater. (2020) 1–6.
[82] Y. Huang, N. Bu, Y. Duan, Y. Pan, H. Liu, Z. Yin, Y. Xiong, Nanoscale 5 (2013) 12007–12017.
[83] J. Doshi, D.H. Reneker, Electrospinning process and applications of electrospun fibers, in: Conference Record of the 1993 IEEE Industry Applications Conference Twenty-Eighth IAS Annual Meeting, IEEE, 1993, pp. 1698–1703.
[84] J.M. Deitzel, J.D. Kleinmeyer, J.K. Hirvonen, N.B. Tan, Polymer 42 (2001) 8163–8170.
[85] Y. Shin, M. Hohman, M. Brenner, G. Rutledge, Polymer 42 (2001) 09955–09967.
[86] P. Wen, M.-H. Zong, R.J. Linhardt, K. Feng, H. Wu, Trends Food Sci. Technol. 70 (2017) 56–68.
[87] H. Asadi, A. Ghaee, J. Nourmohammadi, A. Mashak, Int. J. Polym. Mater. Polym. Biomater. 69 (2020) 173–185.
[88] H.S. Sofi, A. Abdal-Hay, S. Ivanovski, Y.S. Zhang, F.A. Sheikh, Mater. Sci. Eng. C (2020), 110756.
[89] J. Baek, E. Lee, M.K. Lotz, D.D. D'Lima, Biol. Med. 23 (2020), 102090.
[90] H. Rostamabadi, E. Assadpour, H.S. Tabarestani, S.R. Falsafi, S.M. Jafari, Trends Food Sci. Technol. (2020).
[91] M.D.A. Porto, J.P. dos Santos, H. Hackbart, G.P. Bruni, L.M. Fonseca, E. da Rosa Zavareze, A.R.G. Dias, Int. J. Biol. Macromol. 126 (2019) 834–841.
[92] P. Chuysinuan, T. Thanyacharoen, S. Techasakul, S. Ummartyotin, J. Sci. Adv. Mater. Devices 3 (2018) 175–180.
[93] R. Korehei, J.F. Kadla, Carbohydr. Polym. 100 (2014) 150–157.
[94] S. Saha, A. Bhattacharjee, S.H. Rahaman, S. Ray, M.K. Marei, H. Jain, J. Chakraborty, Int. J. Appl. Glass Sci. 11 (2020) 320–328.
[95] R.P. Reksamunandar, D. Edikresnha, M.M. Munir, S. Damayanti, Procedia Eng. 170 (2017) 19–23.
[96] N. Aghamohamadi, N.S. Sanjani, R.F. Majidi, S.A. Nasrollahi, Mater. Sci. Eng. C 94 (2019) 445–452.
[97] I. Solaberrieta, A. Jiménez, I. Cacciotti, M.C. Garrigós, Polymers 12 (2020) 1323.
[98] S. Afshar, S. Rashedi, H. Nazockdast, M. Ghazalian, Int. J. Biol. Macromol. 138 (2019) 1130–1137.
[99] A. Tampau, C. González-Martinez, A. Chiralt, J. Food Eng. 214 (2017) 245–256.
[100] A. Esmaeili, M. Haseli, Carbohydr. Polym. 173 (2017) 645–653.
[101] H.-S. Jung, M.H. Kim, J.Y. Shin, S.R. Park, J.-Y. Jung, W.H. Park, Carbohydr. Polym. 193 (2018) 205–211.
[102] M. Rostami, M. Ghorbani, M. Delavar, M. Tabibiazar, S. Ramezani, Int. J. Biol. Macromol. 135 (2019) 698–705.
[103] L.M. Fonseca, J.P. de Oliveira, P.D. de Oliveira, E. da Rosa Zavareze, A.R.G. Dias, L.-T. Lim, Food Res. Int. 116 (2019) 1318–1326.
[104] Z.-y. Qin, X.-W. Jia, Q. Liu, B.-h. Kong, H. Wang, Int. J. Biol. Macromol. 137 (2019) 224–231.
[105] Y. Jung, H. Yang, I.-Y. Lee, T.-S. Yong, S. Lee, Polymers 12 (2020) 243.
[106] I. Kutzli, M. Gibis, S.K. Baier, J. Weiss, Food Hydrocoll. 93 (2019) 206–214.
[107] Y. Omori, T. Gu, L. Bao, Y. Otani, T. Seto, Aerosol Sci. Technol. 53 (2019) 1149–1157.
[108] H. Liu, S. Zhang, L. Liu, J. Yu, B. Ding, Adv. Funct. Mater. 30 (2020) 2002361–2002369.
[109] S. Zhang, H. Liu, N. Tang, S. Zhou, J. Yu, B. Ding, Adv. Mater. (2020), 2002361.
[110] R.S. Barhate, S. Ramakrishna, J. Memb. Sci. 296 (2007) 1–8.
[111] M. Hashmi, S. Ullah, I.S. Kim, Curr. Res. Biotechnol. 1 (2019) 1–10.
[112] X. Huang, T. Jiao, Q. Liu, L. Zhang, J. Zhou, B. Li, Q. Peng, Sci. China Mater. 62 (2019) 423–436.
[113] X. Tian, B. Xin, W. Gao, S. Jin, Z. Chen, J. Text. Inst. 110 (2019) 815–821.
[114] S.A.A.N. Nasreen, S. Sundarrajan, S.A.S. Nizar, R. Balamurugan, S. Ramakrishna, Membranes 3 (2013) 266–284.
[115] W. Liang, Y. Xu, X. Li, X.-X. Wang, H.-D. Zhang, M. Yu, S. Ramakrishna, Y.-Z. Long, Nanoscale Res. Lett. 14 (2019) 361–370.
[116] S. Lee, A.R. Cho, D. Park, J.K. Kim, K.S. Han, I.-J. Yoon, M.H. Lee, J. Nah, ACS Appl. Mater. Interfaces 11 (2019) 2750–2757.
[117] V. Liwanag, A Reusable Nanofiber Mask Ensuring High Breathability (2020).
[118] Guoxu Liu, Jinhui Nie, Changbao Han, Tao Jiang, Zhiwei Yang, ACS Appl. Mater. Interfaces 10 (2018) 7126–7133.
[119] G.-H. Zhang, Q.-H. Zhu, L. Zhang, F. Yong, Z. Zhang, S.-L. Wang, Y. Wang, L. He, G.-H. Tao, Nat. Commun. 11 (2020) 1–10.
[120] B. Ghatak, S. Banerjee, S.B. Ali, R. Bandyopadhyay, N. Das, D. Mandal, B. Tudu, arXiv preprint arXiv (2005) 1–21, 08305 (2020).
[121] A. Barhoum, H. Li, M. Chen, L. Cheng, W. Yang, A. Dufresne, Handbook of Nanofibers, Springer, New York, 2018, pp. 1–26.
[122] X. Li, S. Teng, X. Xu, H. Wang, F. Dong, X. Zhuang, B. Cheng, Fibers Polym. 19 (2018) 775–781.
[123] M. Faccini, C. Vaquero, D. Amantia, J. Nanomater. 2012 (2012) 892894–892903.
[124] D.B. Dwyer, N. Dugan, N. Hoffman, D.J. Cooke, M.G. Hall, T.M. Tovar, W. E. Bernier, J. DeCoste, N.L. Pomerantz, W.E. Jones Jr, ACS Appl. Mater. Interfaces 10 (2018) 34585–34591.
[125] J. Sheng, J. Zhao, X. Yu, L. Liu, J. Yu, B. Ding, Electrospun Nanofibers for Waterproof and Breathable Clothing, Electrospinning: Nanofabrication and Applications, Elsevier, 2019, pp. 543–570.
[126] Y. Liang, J. Ju, N. Deng, X. Zhou, J. Yan, W. Kang, B. Cheng, Appl. Surf. Sci. 442 (2018) 54–64.
[127] D. Kharaghani, M.Q. Khan, A. Shahzad, Y. Inoue, T. Yamamoto, S. Rozet, Y. Tamada, I.S. Kim, Nanomaterials 8 (2018) 461–473.
[128] N.R. Dhineshbabu, G. Karunakaran, R. Suriyaprabha, P. Manivasakan, V. Rajendran, Nano-micro Lett. 6 (2014) 46–54.
[129] M.H. Mohraz, F. Golbabaei, I.J. Yu, M.A. Mansournia, A.S. Zadeh, S.F. Dehghan, Int. J. Environ. Sci. Technol. 16 (2019) 681–694.
[130] NanoHack: https://copper3d.com/hackthepandemic/, 2020.
[131] R. Tino, R. Moore, S. Antoline, P. Ravi, N. Wake, C.N. Ionita, J.M. Morris, S. J. Decker, A. Sheikh, F.J. Rybicki, COVID-19 And the Role of 3D Printing in Medicine, Springer, 2020.
[132] Kvatthro, HEPA Mask:https://www.thingiverse.com/thing:4222563, 2020.
[133] The Lowell Makes Mask, 2020. https://lowellmakes.com/covid-19-response.
[134] Flexible Mask Valvy, 2020. https://www.thingiverse.com/thing:4177128.
[135] G.R. Swennen, L. Pottel, P.E. Haers, Int. J. Oral Maxillofac. Surg. (2020) 673–677.
[136] D. Liu, T. Koo, J. Wong, Y. Wong, K. Fung, Y. Chan, H. Lim, Anaesthesia 75 (2020) 1022–1027.
[137] J. Cao, Z. Cheng, L. Kang, M. Lin, L. Han, RSC Adv. 10 (2020) 20155–20161.

[138] H. Liu, J. Huang, J. Mao, Z. Chen, G. Chen, Y. Lai, Iscience 19 (2019) 214–223.
[139] H. He, M. Gao, B. Illés, K. Molnar, Int. J. Bioprinting 6 (2020) 278–287.
[140] G. Fortunato, Hello Mask, 2020. https://www.empa.ch/web/s604/schutzmaske.
[141] A.L. Allison, E. Ambrose-Dempster, D. T Aparsi, M. Bawn, M. Casas Arredondo, C. Chau, K. Chandler, D. Dobrijevic, H. Hailes, P. Lettieri, (2020).
[142] J. Zhang, S. Gong, C. Wang, D.Y. Jeong, Z.L. Wang, K. Ren, Macromol. Mater. Eng. 304 (2019) 1900259–1900267.
[143] Q. Zhang, Q. Li, L. Zhang, S. Wang, D.P. Harper, Q. Wu, T.M. Young, Chem. Eng. J. 99 (2020) 125768–125800.
[144] O. Das, R.E. Neisiany, A.J. Capezza, M.S. Hedenqvist, M. Försth, Q. Xu, L. Jiang, D. Ji, S. Ramakrishna, Sci. Total Environ. 736 (2020) 139611–139643.
[145] P. Kenney, O. Hilberg, H. Pedersen, O.B. Nielsen, T. Sigsgaard, J. Allergy Clin. Immunol. 133 (2014), 1477-1480.e1413.
[146] V.V. Kadam, L. Wang, R. Padhye, J. Ind. Text. 47 (2018) 2253–2280.
[147] T.T. Han, L. Yang, K.-B. Lee, G. Mainelis, Aerosol. Air Qual. Res. 18 (2018) 2064–2076.
[148] P. Srikrishnarka, V. Kumar, T. Ahuja, V. Subramanian, A.K. Selvam, P. Bose, S. K. Jenifer, A. Mahendranath, M.A. Ganayee, R. Nagarajan, ACS Sustain. Chem. Eng. 21 (2020) 7762–7773.

Zhenfang Zhang received his Master`s degree at Xi`an Polytechnic University. He is currently working with Prof. Seeram Ramakrishna and Dr. Dongxiao Ji at National University of Singapore. His research includes smart wearables, electrospinning, and 3D printing.

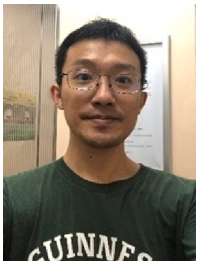

Dongxiao Ji is a research fellow in department of mechanical engineering at National University of Singapore. He received his M.S. and pH.D. degrees in textile science and engineering from Donghua University in 2012 and 2018, respectively. Dr. Ji is experienced in experimental and analytical research work on heterogeneous catalysis, functional nanofibers, and large-scale electrospinng. His research interests include smart/electronic textiles, functional electrospinning membranes, heterogeneous catalysis, and surface modification for environmental and energy applications.

Haijun He is currently a pH.D. student at the Department of Polymer Engineering, Budapest University of Technology and Economics in Hungary. He obtained his B.Sc. and M.Sc. degree in Textile Engineering and Textile Materials at Xi'an Polytechnic University (in China) in 2014 and 2017, respectively. He started his pH.D. study with the Stipendium Hungaricum Scholarship funded by the Tempus Public Foundation (in Hungary) and China Scholarship Council (in China) in 2017. His research interests are in the development of new electrospinning methods for the scale-up of the nanofiber productivity, polymeric composites reinforced with nanofibers, 3D printing, and smart/functional nanomaterials.

Seeram Ramakrishna is a professor in department of mechanical engineering at National University of Singapore. He is a Highly Cited Researcher in Materials Science (Clarivate Analytics, 2014; 2015; 2016; 2017; 2018), and in 'Cross-Field' category (2019). A European study placed him among the only 500 researchers in the world with H-index above 150 in the history of science and technology. He is the world's foremost scientist on nanomaterials by electrospinning for uses in diverse fields such as healthcare, energy, water, and environment. His research work over the past three decades led to seminal contributions in novel processing and mechanistic understanding of functional behavior of composite materials, nanofibers, and nanoparticles. He co-authored ~ 1400 SCI peer reviewed papers which received over 100,000 citations and 150 H-index.